Mathematical modelling of fresh water plumes in fjords

Submitted in partial fulfillment of the requirements of

Master of Science in

Applied and Computational Mathematics

Dereje Beyene

Department of Mathematics

University of Bergen

February 15, 2020

Acknowledgment

First of all I would like to express my deepest gratitude to my supervisor professor Guttorm Alendal for suggesting the topic of this thesis and his endless advice and guidance over the years. It is a great honour to work under his supervision.

I would also like to thank my student advisor Kristine Lysnes whom she has been always in support of my thesis submission deadline extensions.

Finally, I extend my sincere and affectionate gratitude to my beloved wife, Tigist for being always by my side encouraging and supporting throughout this entire study and to our two lovely kids Elana and Lukas for bringing us so much joy all along the way.

Abstract

Nutrients are basic elements for healthier biological process in the ocean.The waters in parts of the fjord like some of the worlds coastal areas doesn't experience exchange between the coast and nutrient and oxygen rich bottom waters. Due to shallow inlet, replacement of water becomes very limited. Pollution from the aquaculture industry, has also played a role in low level oxygen at the bottom (Soltveit and Jensen, 2017).

The main purpose of this thesis is to show ways on how to improve the conditions of the low quality water by entraining and mixing of the waters from the bottom of the sea. One of the different mechanisms that would help in achieving this, is to discharge fresh waters down to the bottom of the fjord. This can create a movement between the waters so that nutritious rich water from the bottom entrained and the over all water quality improved. To get this, buoyant plume model is an effective mechanism since it can entrain large volume of fresh water and mix it with an ambient fluid (Fischer et al., 1979).

A mathematical model has been made for the prediction of spreading and rising of a round buoyant fresh water plume in uniformly stratified stagnant fluid. The model is based on the governing equation of volume, momentum and buoyancy fluxes. The integral equations has been derived in radial and vertical directions using axi-symmetric assumptions. In order to get closure, the basic entrainment assumption has been tested for different values of entertainment constant. The amount of waters entrained from the surrounding in per unit area is of a great interest, since it helps in the design of the over all time needed to transport all the nutrients from the bottom of the water. The maximum vertical distance traveled by the plume is calculated and analyzed for a range of initial parameters when the fresh water hits the linearly stratified fluid. The effects of linear stratification on the plume has also been studied. The model is based on initially round, buoyant plume discharged continuously into stagnant and uniformly stratified water. Mathematical modeling of the plume has been formulated and developed using Matlab ODE 45.

Table of Contents

List of Figures

List of Tables

Notations

α	Entrainment constant
α_p	Round plume entrainment coefficient
α_{jet}	Round jet entrainment coefficient
$\bar{w}$	Vertical top hat plume velocity
λ	Characteristics radius of concentration profile
$\mathcal{F}$	Velocity profile of plume function
$\mathcal{G}$	Concentration profile of plume function
ν	Fluid viscosity
$\overline{v'}$	Average fluctuating radial fluid velocity
$\overline{w'}$	Average fluctuating vertical fluid velocity
ρ	Fluid density
ρ_a	Ambient fluid density
ρ_a	Source fluid density
$\mathbf{u}$	Total plume velocity
b	Plume width
b_c	Plume width defined by concentration
b_G	Gaussian radius
b_v	Plume width defined by velocity
c	Vertical concentration
c_m	Mean vertical concentration
F	Buoyancy flux
F_0	Intitial source buoyancy
Fr	Froude number

g	Gravity
g'	Reduced gravity
h_e	Spreading layer thickness
l_s	Length scale
M	Momentum flux
M_0	Initial momentum flux
M_n	Neutral buoyancy level momentum flux
N^2	Square of buoyancy frequency
p	Pressure
p_∞	Ambient fluid pressure
Q	Volume flux
Q_0	Initial volume flux
Q_e	Flow entrainmnet into the plume
Q_n	Neutral buoyancy level volume flux
Q_{max}	Maximum volume flux
r	Radial distance
R_e	Reynolds number
t	Time
V	Radial fluid velocity
v	Radial mean velocity
v'	Fluctuating radial velocity component
v_e	Entrainment velocity
W	Vertical fluid velocity
w	Vertical velocity
w'	Fluctuating vertical fluid velocity
w_A	Vertical velocity at point A
w_B	Vertical velocity at point B
w_m	Mean vertical velocity
w_n	Vertical velocity at neutral buoyancy level

x	horizontal coordinate
z	Elevation above the source
z_h	Neutral buoyancy level height
z_m	Maximum height

Chapter 1

Introduction

1.1 Basic concepts of jets and plumes

The main difference between jets and plumes is that in jets flow is produced by continuous momentum sources whereas in plumes the flow is driven by buoyancy sources. For instance the high velocity flow in a pipe can be considered as a jet while a smoke from a rising fire forms a plume. Despite the fluid is discharged as a jet where the force of buoyancy (which is the result of the density difference between the discharged and the ambient fluids) is not dominant, it eventually changed in to plumes given enough distance from the source. Both of jets and plumes can be laminar or turbulent. In the next two subsections, the detailed description of each of the classifications will be presented.

1.1.1 Jets

A jet is the flow of fluid into a surrounding medium of the same or similar fluid (Fischer et al., 1979). Turbulent jets are a very common feature in many waste disposal system design such as heating or cooling towers effluent disposal into the ocean (Fischer et al., 1979). They also occur naturally in "black smokers" which is released from deep sea hydrothermal vents(Lee and Chu, 2003). The flow in a jet near at the discharge point is controlled by the initial conditions such as exit velocity, turbulence intensity and velocity distribution. Mostly the initial flow is driven by the momentum of the fluid at the discharge point. Since velocity is momentum per unit mass, any means of producing velocity is a momentum force (Lee and Chu, 2003). Many laboratory experiments show that when Reynolds number which is defined as $R_e = 2w_0b/\nu$ is greater than 2000, the jet become turbulent (Lee and Chu, 2003). Where w_0, b and ν are exit velocity, source radius and fluid viscosity respectively.

1.1.2 Plumes

A flow in a plume is somewhat similar to that of a jet except it is driven by the force of buoyancy which is a potential source of energy that provides the fluid with positive or negative buoyancy with respect to the surrounding environment Fischer et al. (1979). Many physical processes can be the cause for the change in the density of the fluid (Fischer et al., 1979). Plumes can be either laminar or turbulent flow

in nature. If Reynolds number which is a transition from laminar to turbulent, is sufficiently high, then the flow becomes fully turbulent. When both momentum and buoyancy are present at the source, it classified as buoyant jets. Near the source in buoyant jets, momentum is the dominant force. But buoyancy is a significant factor in some cases at the source when the momentum created by the buoyancy force is greater than the initial momentum force.

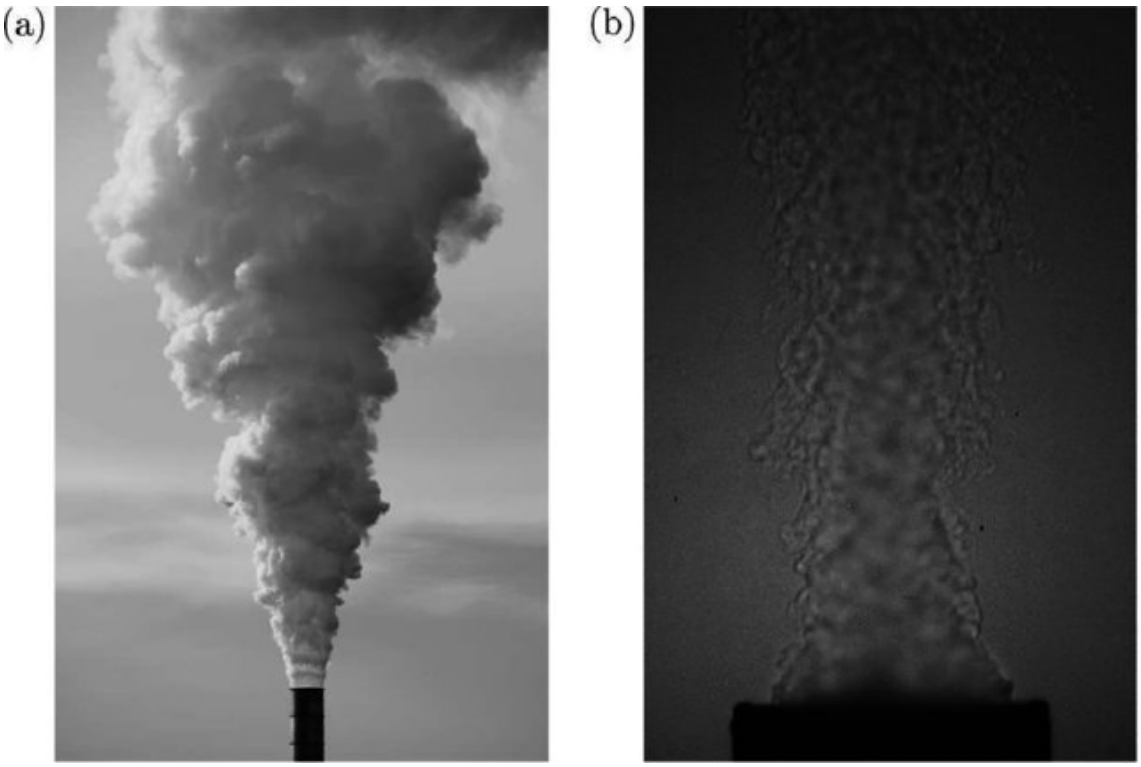

Figure 1.1: (a) A vapour plume above an industrial smoke stack. (b) An inverted shadowgraph image of a saline plume (Source: Oxford University)

1.1.3 Plume classifications

A flow generated by a finite source of mass and excessive momentum flux is called forced plumes (Morton, 959b). Plumes are classified based on non-zero initial volume, momentum and buoyancy fluxes at the source as :

$$\Gamma_0 = \frac{5F_0Q_0^2}{\alpha\sqrt{16\pi}M_0^{5/2}} \tag{1.1}$$

where Q_0, M_0 and F_0 are the initial volume, momentum and buoyancy fluxes. Whereas α is the entrainment constant (refer to Section 2.1.3). When $\Gamma_0 = 1$, the plume is called pure plumes as the volume and momentum fluxes are in balance. The plumes are called lazy plume when there is less momentum flux with the same amount of volume and buoyancy fluxes as $\Gamma_0 > 1$. The plumes become forced plume when Γ_0 is less than one. Plumes are also classified depending on the direction of the initial momentum and buoyancy fluxes. When they are in the same direction, it is called positively buoyant plumes. The plumes in this case is dominated by momentum at the source while the force of buoyancy dominates far from the source. When the

initial momentum and buoyancy fluxes are in opposite direction, the plumes is called negatively buoyant plume.

1.2 Related literature overview

The models for the characteristics of turbulent buoyant jets and plumes has been studied since 1930s. The foundation work on plumes which includes the mixing of the surrounding fluids in to the plume was laid by Zeldovich (1937) and later on by Morton et al. (1956).

Experimental studies of plumes in stagnant ambient fluid by Rouse et al. (1952) showed that the velocity profile exhibited a Gaussian distribution and the width of the plume expanded linearly with the height of the plume.

The classic and remarkable paper that shows a different integral models for solving plume model problems in uniformly stratified environment was done by (Morton et al., 1956). For the first time, they introduced the idea of entrainment hypothesis which is a solution for closure of turbulent flow equations. The exact value of its entrainment coefficient has become an open question since then. They wrote a series of equations for the conservation of volume, momentum and buoyancy flux for stratified environment. These conservation equations have considered Boussinesq plumes which is the density difference between the plume and the fluid into which they are submerged. In Boussinesq approximation, the density difference wouldn't be considered except when it is multiplied by gravity. These equations are discussed in detail in Chapter 2. The study of forced plumes was conducted by Abraham (1963) in his doctoral thesis. He assumed the plume spreads horizontally at a certain rate questioning the use of constant entertainment coefficient by (Morton, 959b).

In all the previous cases the environment is assumed to be uniformly stratified. The case of non-uniformly stratified environment for turbulent plumes was examined by (Caulfield and Woods, 1998). They found that if the stratification decayed rapidly enough, no matter how the environment stratified, the plume will continue rising indefinitely without reaching a neutral buoyancy level. Analytical solution for a point source forced plume in uniformly stratified environment has been developed by (Wong and Wright, 1988). In an experimental study, they measured terminal dilution and predicted maximum rise height of the plume.

1.3 Thesis objectives

The basin waters in parts of the fjords is becoming oxygen depleted because of lack of replacement of nutrients and oxygen rich bottom and the coast waters (Soltveit and Jensen, 2017). The deep water renewal process is a phenomena that overcome this problem. This can be triggered by natural or artificial upwelling. Naturally the water renewal takes place when the coastal water above sill level is denser than the deep water. Because of the density difference, the deep water goes to the bottom, while the deep water is lifted to higher levels. This inflow creates turbulence that can generate mixing of the new water with the adjacent waters. If such diffusive vertical exchange continues, stratification of the basin decreases in time which leads to advective water exchange (Aure and Stigebrandt, 1989).

According to Aure and Stigebrandt (1989) stagnation periods occur when advective processes couldn't drive the water renewal process, though vertical diffusion may also involve the biological consumption of oxygen which is somewhat equal to the decay rate of oxygen. Upwelling nutritious water from deep ocean to the near surface water increases primary production since it brings the nutrient-rich, deep ocean water to the euphotic zone which increases the total nutrient concentrations and enhance mariculture (Yiwen et al., 2016). Although it's only 0.1% of the sea surface where the natural upwelling occurs, the quantity of fishes produced there occupies more than half of all products of fishes in the world (Nagamatsu and Shima, 2006).

The main purpose of this thesis is to build a mathematical model that can entrain and mix the water from the bottom of the fjords which helps in improving the conditions of the low quality water. The model is based on the assumption of discharging fresh water from bottom of the fjord. This mechanism is called artificial upwelling. Many studies on artificial upwelling mechanisms are made for enhancing mariculture so far (Golmen, 1998).There are two ways to do artificial upwelling the deep sea water. One way is by using a pump and another is to make special underwater structures[1] on the bottom of the sea for upwelling Nagamatsu and Shima (2006). According to McClimans et al. (2002) and the density profiles in Appendix A.3, there is a reasonable linear stratification in parts of the fjord. In such cases fresh water can be used down to the bottom of the sea. Hence, the plume emerges upward direction because of the density difference between the submerged water and the environment. The developed model has also been tested in Section 2.7 for the sensitivity of the predictions to variations in entrainment coefficient and buoyancy frequency.

[1]Special underwater structures that put on the sea bottom includes fence, V-shaped structure and mount. These structures are advantageous in relation to less maintenance costs and need no power supply (Nagamatsu and Shima, 2006).

Chapter 2

Mathematical formulations of the plume model

2.1 Introduction

A round plume is driven by the continuous force of buoyancy caused by the density difference between the discharging fluid and the surrounding fluid. The initial state of motion then changed eventually into turbulence and the flow spreads radially by entraining ambient fluid. For the round plume, as is shown in Figure 2.1, where considering the dimension of the source and initial momentum flux, the maximum vertical velocity and the buoyancy field at the source can be related as (Batchelor, 1954):

$$w_m = \left(\frac{F_0}{z}\right)^{1/3} f(r/z) \tag{2.1}$$

where F_0 is initial buoyancy of the plume which is produced by discharging fluid of density ρ_0 and z is the vertical distance from the source. In the same way according to Batchelor (1954), the maximum vertical concentration and the mass flux at the source can be related as

$$c_m = F_0^{2/3} z^{-5/3} g(r/z). \tag{2.2}$$

Many experiments have been done to relate the variable r/z with the above function $\mathcal{F}$ and $\mathcal{G}$. In many of the cases, the approximation of these data assumes a Gaussian profile of the form

$$\mathcal{F}(r/z) = e^{-\frac{r^2}{b^2}} \tag{2.3}$$

$$\mathcal{G}(r/z) = e^{-\frac{r^2}{(\lambda b)^2}} \tag{2.4}$$

where b is the width of the plume while λb is the width for the concentration profile. As one can see, the width of the concentration profile is wider in small degree by a factor λ compared with the width of the velocity profile, b. According to the data from Papanicolaou and List (1988), the width of the plume increases linearly away from the source with $b = 0.105z$.

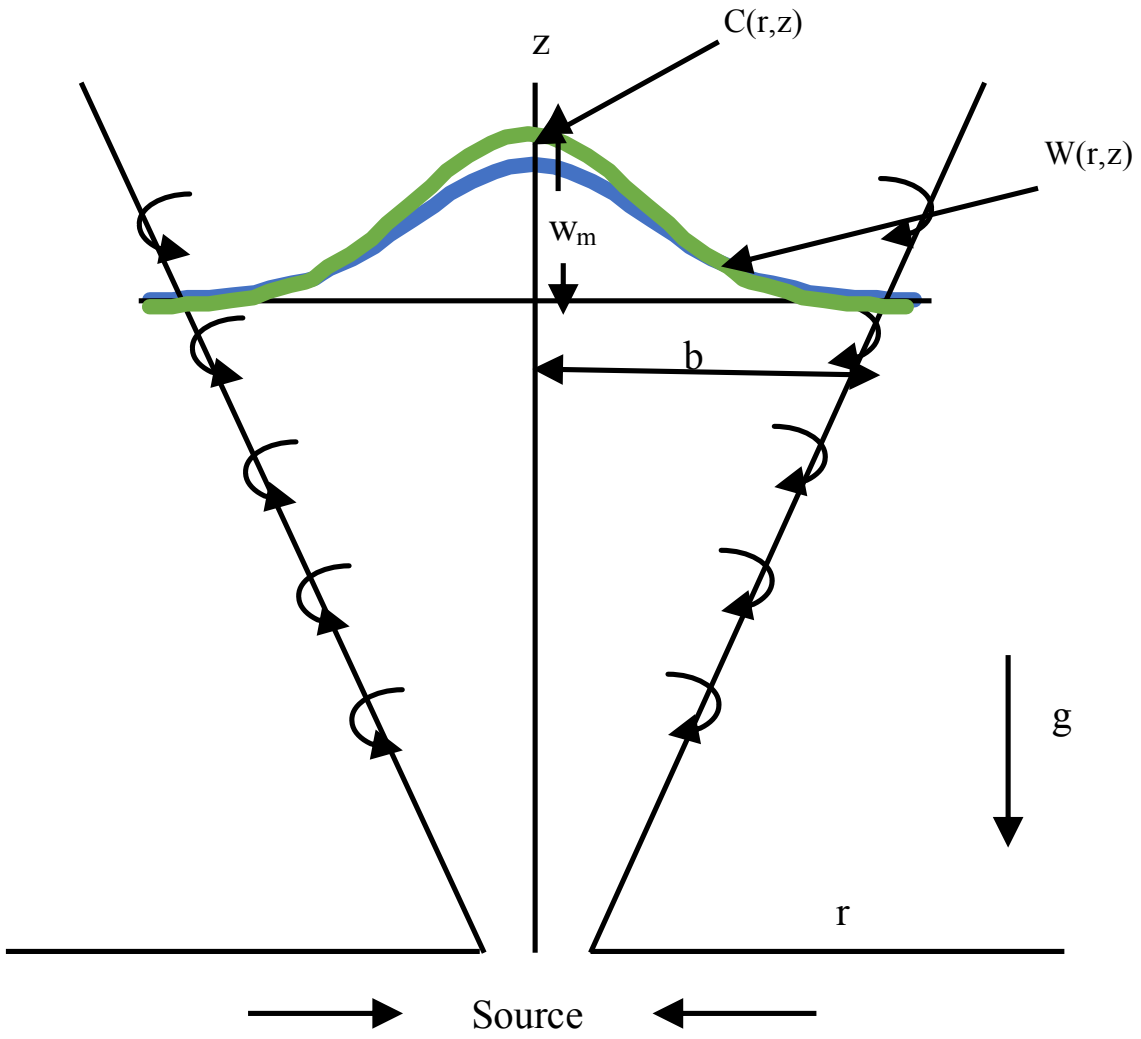

Figure 2.1: Schematic of velocity and concentration profile in a round plume.

2.1.1 Governing equations

The general flow equations for an inviscid fluid in a Cartesian coordinates can be written as Yih (2012).

$$\rho\Big(\frac{\partial v_i}{\partial t} + v_\alpha \frac{\partial v_i}{\partial x_\alpha}\Big) = -\frac{\partial p}{\partial x_i} \tag{2.5}$$

where ρ is density of the fluid, p is pressure, t is time and v_i is velocity component along x_i. With (i = *1, 2, and 3*), repeated indices in the equation indicates Einstein

summation convention. This implies that,

$$v_\alpha \frac{\partial v_i}{\partial x_\alpha} = v_1 \frac{\partial v_i}{\partial x_1} + v_2 \frac{\partial v_i}{\partial x_2} + v_3 \frac{\partial v_i}{\partial x_3} \tag{2.6}$$

Considering a vertical axisymmetric of an incmpressible flow of a cylindrical coordinates system with no variability in θ [1], the velocity and concentration profile can be given by:

$$\begin{aligned} w(z,r) &= w_m(z) e^{-(\frac{r}{b})^2} \\ c(z,r) &= c_m(z) e^{-(\frac{r}{\lambda b})^2} \end{aligned} \tag{2.7}$$

where w_m and c_m are the maximum vertical velocity and concentration, and b is plume radius. Considering vertical axisymmetric cylindrical coordinates system, the radial momentum equation becomes (Schlichting, 1979):

$$\rho\Big(\frac{\partial V}{\partial t} + V\frac{\partial V}{\partial r} + W\frac{\partial V}{\partial z}\Big) = -\frac{\partial p}{\partial r} \tag{2.8}$$

where V and W are the velocity components in the radial r and vertical z directions, respectively. According to Schlichting (1979), the vertical momentum for the vertical axisymmetric cylindrical coordinates system is

$$\rho\Big(\frac{\partial V}{\partial t} + V\frac{\partial W}{\partial r} + W\frac{\partial W}{\partial z}\Big) = -\frac{\partial p}{\partial z} - g\rho \tag{2.9}$$

The continuity equation can be written as

$$\frac{\partial \rho}{\partial t} + \nabla.(\rho \mathbf{u}) = 0 \tag{2.10}$$

where $\mathbf{u}$ is the velocity field in cylindrical coordinates system and defined as $\mathbf{u} = (V, 0, W)$. After substitution and simple rearrangement, Equation 2.10 becomes

$$\frac{1}{\rho}\frac{\partial \rho}{\partial t} + \frac{\partial V}{\partial r} + \frac{\partial W}{\partial z} = 0 \tag{2.11}$$

For an incompressible fluid, $\frac{1}{\rho}\frac{\partial \rho}{\partial t} << 1$, so Equation 2.11 becomes:

$$\frac{1}{r}\frac{\partial (rV)}{\partial r} + \frac{\partial W}{\partial z} = 0. \tag{2.12}$$

Both the vertical and radial velocities vary in time because of turbulent fluctuations, so the velocity is decomposed in to a mean and a turbulent component, i.e the traditional Reynolds decomposition. For V and W the Reynolds decomposition

[1] Assuming a cylindrical coordinates plane, θ is the angle between the reference direction on the plane and the line from the origin to the projection of the point on the plane

would be

$$\begin{aligned} V &= v + v' \\ W &= w + w' \end{aligned} \tag{2.13}$$

where v and w are the time averaged part where as v' and w' are the fluctuating parts. With this and taking the mean of each terms, Equation 2.12 becomes

$$\frac{1}{r}\frac{\partial(rv)}{\partial r} + \frac{\partial w}{\partial z} = 0. \tag{2.14}$$

Substituting the Reynolds decomposition into Equation 2.8 and taking the mean of each terms in the equation, the radial momentum equation is then,

$$\rho\left(v\frac{\partial v}{\partial r} + w\frac{\partial v}{\partial z}\right) = -\frac{\partial p}{\partial r} - \rho\left(\frac{\partial\overline{(v')^2}}{\partial r} + \frac{\partial(\overline{v'w'})}{\partial z} + \frac{\overline{v'^2}}{r}\right) \tag{2.15}$$

where the overbar denote the time average of the fluctuating parts. The detailed derivation of the above radial component momentum equation is presented in Appendix **A.1**. By applying the same method, the vertical component of momentum equation then becomes

$$\rho\left(v\frac{\partial w}{\partial r} + w\frac{\partial w}{\partial z}\right) = -\frac{\partial p}{\partial z} - g\rho - \rho\left(\frac{\partial\overline{(w')^2}}{\partial z} + \frac{\partial(\overline{v'w'})}{\partial r} + \frac{(\overline{v'w'})}{r}\right) \tag{2.16}$$

The detailed derivation of Equation 2.16 is found in Appendix **A.2**. Substituting the values of V and W from Equation 2.13 into Equation 2.11 and after some algebra, we end up with

$$v\frac{\partial\rho}{\partial r} + w\frac{\partial\rho}{\partial z} = -\frac{\partial(\overline{\rho'v'})}{\partial r} - \frac{\partial(\overline{\rho'w'})}{\partial z}. \tag{2.17}$$

Equation 2.17 is called density or mass conservation. At this point we refer to the idea of Boussinesq approximation that ignores a small density differences except in the cases when they are multiplied by g, the gravitational acceleration. This approximation helps to consider a single density (In this case we can say that density of the plume is approximately equal to density of the environment, $\rho \approx \rho_a$) which will simplify the derivation of the equations. For a fluid at rest or at zero velocity, it's pressure gradient is balanced by the force of gravity, $\frac{\partial p}{\partial z} = -\rho_a g$. By applying Boussinesq approximation, replacing ρ with a reference density, ρ_0 in all terms except in ρg, most of the time the reference density is the density of the environment at $z = 0$. Then Equation 2.16 in cylindrical coordinates becomes

$$v\frac{\partial w}{\partial r} + w\frac{\partial w}{\partial z} = g' - \frac{\partial\overline{(w')^2}}{\partial z} - \frac{1}{r}\frac{\partial(\overline{rv'w'})}{\partial r}, \tag{2.18}$$

where $g' = \frac{(\rho_a - \rho)}{\rho_0}$ is the reduced gravity. To summarize the continuity equation, radial and vertical momentum equations and mass conservation equation, assuming steady state flow, become

$$\frac{\partial v}{\partial r} + \frac{\partial w}{\partial z} = 0 \tag{2.19}$$

$$v\frac{\partial v}{\partial r} + w\frac{\partial v}{\partial z} = -\frac{1}{\rho}\frac{\partial p}{\partial r} \tag{2.20}$$

$$v\frac{\partial w}{\partial r} + w\frac{\partial w}{\partial z} = -\frac{1}{\rho}\frac{\partial p}{\partial z} - g \tag{2.21}$$

$$v\frac{\partial \rho}{\partial r} + w\frac{\partial \rho}{\partial z} = 0 \tag{2.22}$$

There are two assumptions taken from the boundary conditions of the plume (Lee and Chu, 2003)

i. The velocity in the radial direction is much less than the velocity in the axial direction, $v \ll w$

ii. The partial derivative of the velocity in the axial direction is much less than the velocity in the radial direction; $\frac{\partial}{\partial z} \ll \frac{\partial}{\partial r}$

By applying the boundary-layer conditions in Equation 2.15, which is the radial momentum equation and neglecting small terms, we get

$$p + \rho\overline{(v')^2} \simeq p_\infty \tag{2.23}$$

We see that the above governing equations leads us in which there are more unknowns than equations because of the flow is divided into mean and fluctuation parts. This is called the closure problem of turbulence model and the details may be found in (Tennekes and Lumley, 1994).

2.1.2 Eulerian integral model

One way to achieve the turbulent closure of the plume equations is to integrate the plume equations across the buoyant plume. Multiplying Equation 2.19 by $2\pi r$ and then integrating from $r = 0$ to $r = \infty$ we get

$$\begin{aligned} \frac{d}{dz}\int_0^\infty (w2\pi r)dr &= -\int_0^\infty 2\pi v dr \\ &= -2\pi r v \mid_0^\infty \\ &= Q_e \end{aligned} \tag{2.24}$$

where Q_e is defined as the entrainment flow per unit length. Here the interesting point is that as r goes to ∞, v goes to 0, but as Lee and Chu (2003) put it, rv remains finite. This tells us about the entrainment of flow in to the plume and can be written as $Q_e = 2\pi b v_e$ where v_e is the entrainment velocity at the lateral edge of the plume, $r = b$.

In a similar fashion, Equation 2.18 can be rewritten as

$$rv\frac{\partial w}{\partial r} + rw\frac{\partial w}{\partial z} = rg' - r\frac{\partial \overline{(w')^2}}{\partial z} - \frac{\partial(\overline{rv'w'})}{\partial r} \tag{2.25}$$

Similarly the integral method can be applied on Equation 2.25 across the plume from $r = 0$ to $r = \infty$. Neglecting the fluctuating terms and applying the boundary conditions, we have

$$\frac{d}{dz}\int_0^\infty 2\pi r w^2 dr = \int_0^\infty 2\pi r g' dr. \tag{2.26}$$

The buoyancy force, which is represented by the right hand side equation, is the gravitational force resulting from the difference in density. Whereas, the momentum flux which is represented by the left hand side equation, is due to the buoyancy force in relation to the reduced density across the plume.

By integrating the density conservation in Equation 2.17 from $r = 0$ to $r = \infty$, we get

$$\frac{d}{dz}\int_0^\infty w 2\pi r g' dr = \int_0^\infty w 2\pi r \frac{\rho_a - \rho}{\rho_a} g dr \tag{2.27}$$

The above equation shows us that the buoyancy flux is inversely proportional to height and directly proportional to the density gradient. The governing equations for that we obtained for the integral modes presented as:

$$\frac{d}{dz}\int_0^\infty 2\pi r w dr = 2\pi b v_e \tag{2.28}$$

$$\frac{d}{dz}\int_0^\infty 2\pi r w^2 dr = \int_0^\infty 2\pi r g' dr \tag{2.29}$$

$$\frac{d}{dz}\int_0^\infty 2\pi r w g' dr = \int_0^\infty 2\pi r w \frac{\rho_a - \rho}{\rho_a} g dr \tag{2.30}$$

2.1.3 Entrainment hypothesis

For the closure of the governing equations, additional equation for the entrainment velocity v_e is required. $v_e = \alpha w_m$ where α is the entrainment constant. Morton et al. (1956) proposed the famous classical method for the entrainment assumption.

Before Morton et al. (1956) put the hypothesis, Batchelor (1954) came up with the increasing vertical flow in a plume implies that there is a mean inflow in the vertical velocity. By the simplest assumption which is the entrainment velocity is proportional to the vertical velocity which inturn proportional to the turbulent velocity. After substituting the velocity profile in Equation 2.7 (assuming there is equal spread in velocity and density) into Equation 2.27 to 2.29, the governing equations become

$$\frac{d}{dz}(\pi b^2 w_m) = 2\pi\alpha b w_m \tag{2.31}$$

$$\frac{d}{dz}\left(\frac{\pi}{2} b^2 w_m^2\right) = \pi b^2 g' \tag{2.32}$$

$$\frac{d}{dz}(\pi b^2 w_m g') = -\pi b^2 w_m N^2(z) \tag{2.33}$$

where $N^2(z) = \frac{-g}{\rho_0}\frac{d\rho_a}{dz}$ is the square of the local buoyancy frequency. The exact value of the entrainment coefficient is a matter of an open question. Laboratory measurements of α vary considerably. When the environment is of uniform density, the radial growth, b and α can be related as $b = \frac{6}{5}\alpha z$ (Details can be found in Section 3.1.1). In the presence of buoyancy variation, α is related with bulk flow measurement like in volume flux as $\frac{1}{Q}\frac{dQ}{dz} = 2\frac{\alpha}{b}$ (Turner, 1979). The radial growth rate technique predicts higher value of α than the bulk flow measurement by Kaye (2008). One of the explanations given for this phenomenon by Kaye (2008) is the entrainemnt coefficient is lower in the near field zone and that the bulk flow measurements basically integrate α over the plume height and produce lower value of α than the value gained from measuring the radius of a fully developed flow.

2.1.4 Gaussian profile

Turbulent plume modeling by using Gaussian profile is the most common one since it matches with the already proven experimental data by Scase and Hewitt (2011). According to the data in Figure 2.1.4 obtained from the experiment by Papanicolaou and List (1988), the center-line mean velocity and concentration profiles shows Gaussian distributions such that

$$\frac{w}{w_m} = e^{-(\frac{r}{b})^2} \tag{2.34}$$

$$\frac{g'}{g'_m} = e^{-(\frac{r}{\lambda b})^2}. \tag{2.35}$$

The reduced gravity, which is the buoyancy force per unit mass of the fluid, have the same profile as the concentration of any tracer (Lee and Chu, 2003).

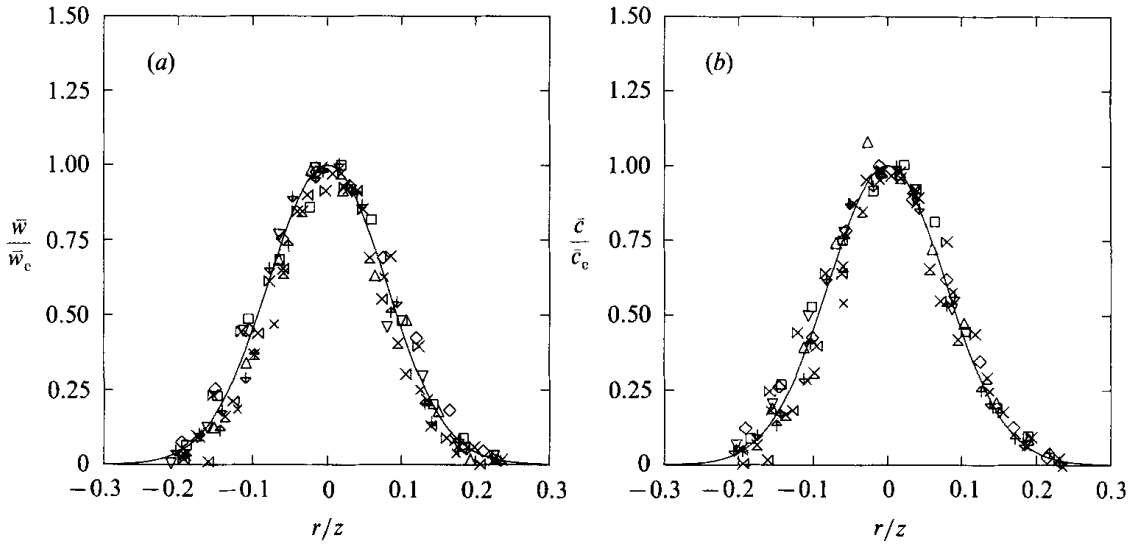

Figure 2.2: Gaussian distribution of measured mean velocity and concentration profile in a round plume ((Papanicolaou and List, 1988))

2.1.5 Top-hat profile

The use of top-hat profile leads to a simpler mathematical derivations. The velocity profile can be defined as:

$$w(r,z) = \begin{cases} \overline{w}(z)_T & \text{if } r \leq b \\ 0 \quad \text{Otherwise.} \end{cases} \tag{2.36}$$

Using top-hat profile integral method the conservation equations might be reduced to the form

$$\frac{d(b^2\overline{w}_T)}{dz} = 2\alpha b\overline{w}_T \tag{2.37}$$

$$\frac{d(b^2\overline{w}_T^2)}{dz} = b^2 g' \tag{2.38}$$

$$\frac{d(b^2\overline{w}_T g')}{dz} = -b^2\overline{w}_T N^2(z) \tag{2.39}$$

where $\overline{w}_T$ is the center-line velocity of a top-hat profile.

2.1.6 Zone of flow establishment

Much work has been done to study the trajectory characteristics of a plume when integrated across its cross section for more than half a century. The development of the plume is divided into the zone of flow establishment (ZFE) and the zone of established flow (ZEF). The distance between the source and the beginning of ZEF, $z < 5.2D_0$ develops from top hat profile at the exit to Gaussian profile at

the beginning of ZEF (Lee and Chu, 2003). In the ZEF, $z > 5.2D_0$, the profile is assumed to be self-similar. This means the trajectory at different height look similar in shape and can be approximated by Gaussian distributions. Assuming the top-hat profile is maintained throughout the trajectory should be taken with a model of equivalent parameters. The volume flux in ZFE zone can be stated as

$$Q_A = \pi b_T^2 w_A \tag{2.40}$$

$$\begin{aligned} Q_B = \int_0^\infty 2\pi r w dr &= \int_0^\infty 2\pi r w_B e^{(-\frac{r^2}{b_G^2})} dr \\ &= \pi w_B b_G^2 \end{aligned} \tag{2.41}$$

where A and B denotes the beginning and end of the ZFE. It is showed in Figure 2.3. Thus the profiles at A are top-hat and at B are Gaussian. b_G is Gaussian radius and w_B is vertical velocity at point B.

By applying the same method, Henderson-Sellers (1983) showed the momentum flux at A and B become

$$M_A = \pi b_T^2 w_A^2 \tag{2.42}$$

$$M_B = \frac{1}{2}\pi w_B^2 b_G^2 \tag{2.43}$$

where b_T is top-hat radius. For a large Froude number $w_A = w_B$ and by equalizing Equations 2.40 and 2.41

$$b_G = \sqrt{2} b_T. \tag{2.44}$$

Hence, the volume flux in Equation 2.41 become

$$Q_B = 2\pi w_B b_T^2. \tag{2.45}$$

In similar ways, the buoyancy fluxes is formulated as

$$F_A = \pi w_A \frac{\rho_a - \rho}{\rho_a} g b_T^2 \tag{2.46}$$

$$\begin{aligned} F_B = \int_0^\infty \frac{\rho_a - \rho}{\rho_a} g 2\pi r dr &= \frac{\pi\lambda^2}{1+\lambda^2} w_B \frac{\rho_a - \rho}{\rho_a} g b_G^2 \\ &= \frac{2\pi\lambda^2}{1+\lambda^2} w_B \frac{\rho_a - \rho}{\rho_a} g b_T^2 \end{aligned} \tag{2.47}$$

where λ is a constant. Thus the volume, momnetum and buoyancy fluxes that has

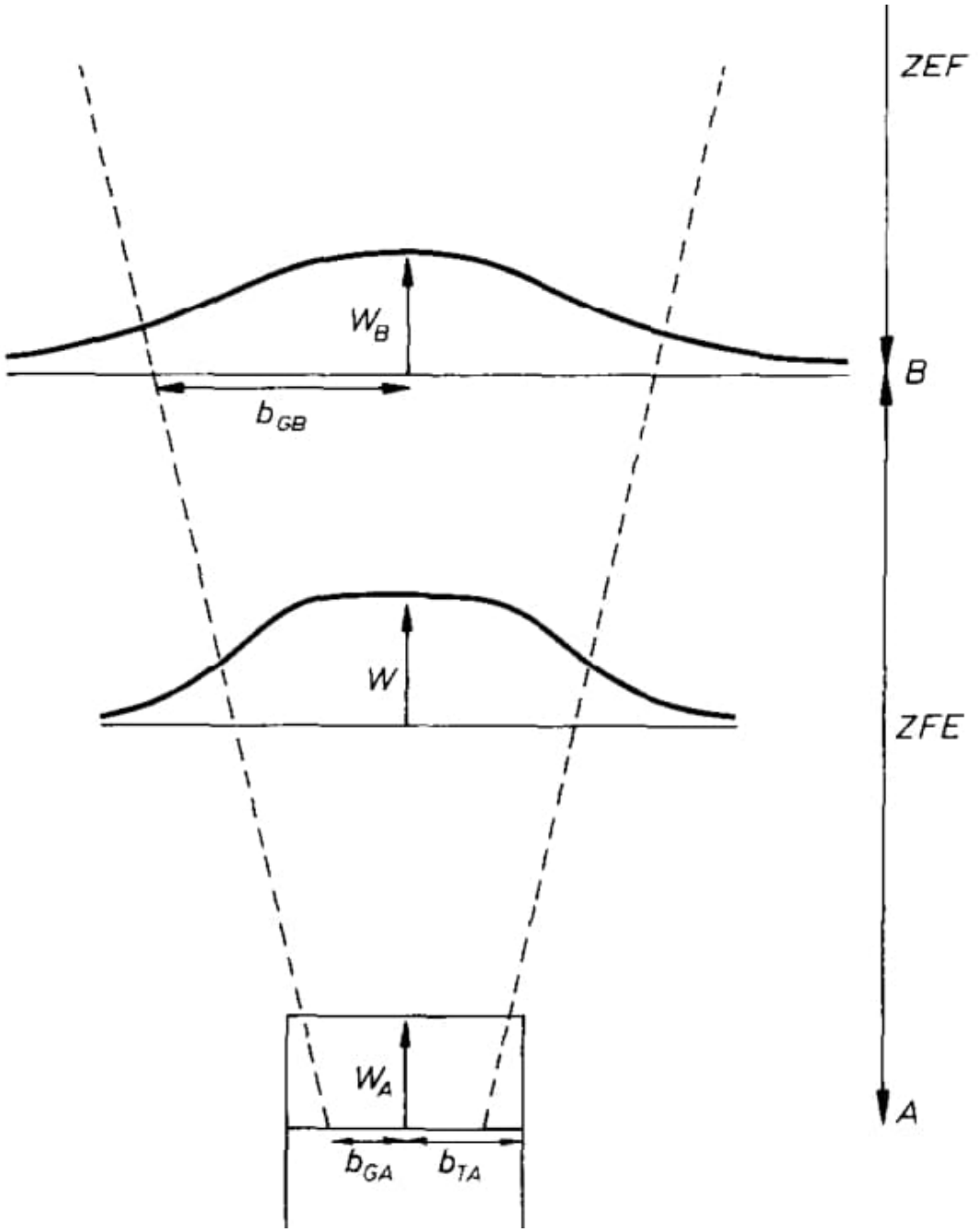

Figure 2.3: Zone of flow establishment (ZFE) and zone of established flow (ZEF) for a plume (Henderson-Sellers (1983))

been defined at the beginning of ZEF occurs approximately at a distance of $5.2D_0$ Lee and Chu (2003).

2.2 Plumes in uniformly stratified environment

In general term, water bodies are density stratified due to salinity, temperature or oxygenation differences. This creates layers with the least dense water sits at the top of dense fluid. If this density difference is linear with depth, then we have a

linear stratification. This stable stratification occasionally disturbed by turbulence. These disturbance might be in the form of momentum and buoyancy which produce a vertical motion which in turn mixes the water layers. Figure 2.4 shows a typical density stratification in Sørfjorden, southern Hordaland county. The plume goes upward as long as the density of the plume is less than the density of the environment, as the same time the buoyancy flux of the plume decreases with height. When the density of the plume reaches at a point equals with the density of the environment, the buoyancy force becomes zero. Though the buoyancy vanishes at a neutral buoyancy level, the plume overshoots to a certain height to form a dome like form due to the momentum. This fluid falls back and spreads radially since it's weight is larger than the surrounding fluid.

As the dome fluid falls back mixing occurs to form a horizontal layer. Many experiments show that the spreading layer is quite thick than the maximum height the plume goes. The maximum height of a plume and the thickness of the horizontal layer can be determined from laboratory experiments. Wong and Wright (1988) provided a formula for the thickness of the horizontal spreading layer as

$$h_e = 1.7 F_0^{\frac{1}{4}} N^{-\frac{3}{4}}. \tag{2.48}$$

Based up on repeated laboratory experiments, Briggs (1970) comes up with the formula for the rise of the plume and is given as

$$z_m = 3.76 F_0^{\frac{1}{4}} N^{-\frac{3}{4}} \tag{2.49}$$

2.3 Integral analysis of the plume equations

A pure plume is where the flow pattern is governed by only the sources of buoyancy where it has zero initial momentum flux and moves in the direction of the buoyancy force. Away from the source, the plume develop increasing momentum flux due to the continuous rise of the buoyant fluid. In a linearly stratified environment, the plume will not continue to rise indefinitely. If the plume is lighter fluid, dispersion and mixing of the plume might occur away from the source.

Morton et al. (1956) has analyzed for the plume rising from a point source driven by buoyant force.

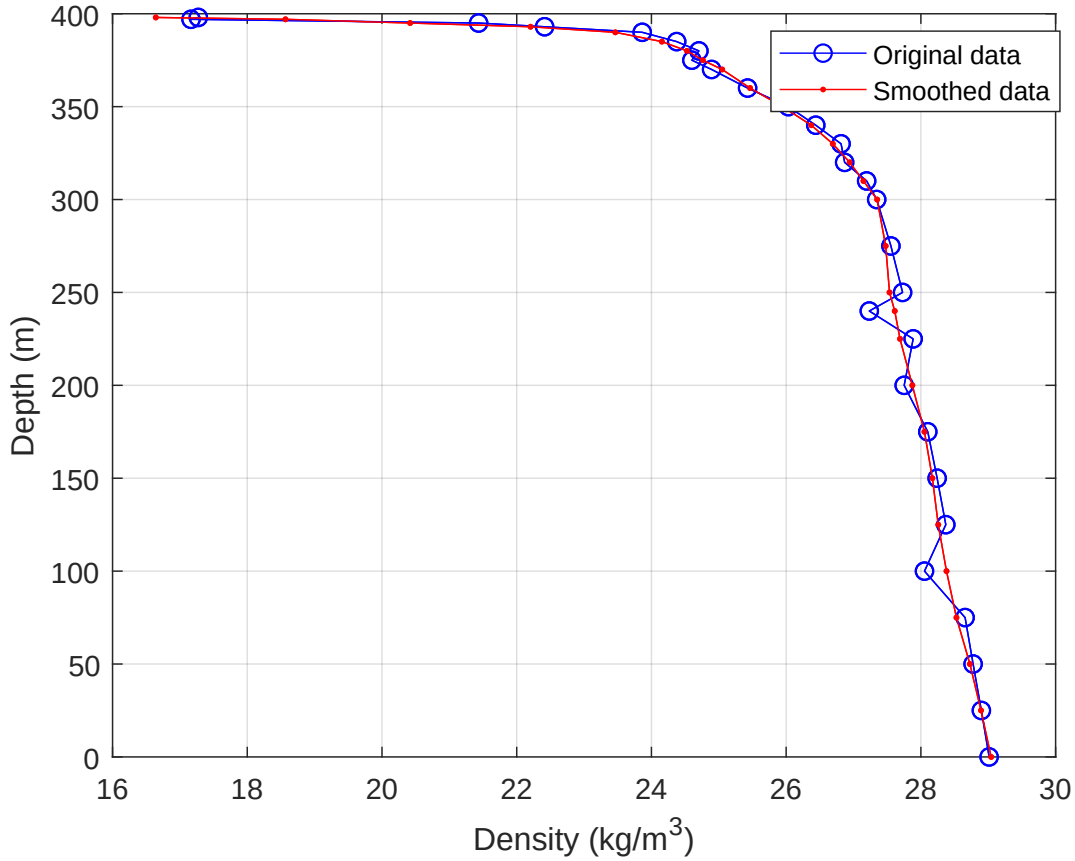

Figure 2.4: The mean density profiles in Sørfjorden. Measurements which is provided by NORCE (Norwegian Research Center) were made between 2011-2016.

2.3.1 Volume flux

As it has described in Subsection 2.1.3, we apply the entrainment hypothesis in order to close the system. By combining this with Equation 2.29 and adopting Top-hat configuration, the volume flux becomes

$$\frac{dQ}{dz} = \frac{d}{dz}\int_0^\infty 2\pi r w dr = 2\pi\alpha b w_m \tag{2.50}$$

2.3.2 Momentum flux

By taking the vertical momentum equation which is derived in Equation 2.18 and assuming steady state flow we will get

$$r\frac{\partial w^2}{\partial z} = rg' \tag{2.51}$$

By integrating both sides with respect to r, the top-hat profile of the momentum flux become

$$\frac{d}{dz}\int_0^b rw^2 dr = \int_0^b rg' dr \tag{2.52}$$

We can re-write Equation 2.52 as:

$$\frac{d}{dz}(b^2 w_m^2) = b^2 g' \tag{2.53}$$

2.3.3 Buoyancy flux

As the plume goes up, the tracer concentration is affected by the change of buoyancy flux. Since the density variation is very small that to be measured directly, the convenient way is to measure it's concentration deficiency or the rate of change of heat. The result from both ways gives us indirect expression of the density deficiency. Integrating Equation 2.27, one gets

$$\frac{d}{dz}(b^2 w_m g') = -b^2 w_m N^2(z) \tag{2.54}$$

The above flux equations can be expressed in terms of the three unknown fluxes. Let's define the three entities as: $Q = b^2 w_m$, $M = b^2 w_m^2$, $F = b^2 w_m g'$. The volume, momentum and buoyancy flux equation become

$$\frac{dQ}{dz} = 2\alpha M^{\frac{1}{2}} \tag{2.55}$$

$$\frac{dM}{dz} = \frac{FQ}{M} \tag{2.56}$$

$$\frac{dF}{dz} = -QN^2(z) \tag{2.57}$$

2.4 Lagrangian plume modeling

Let's consider a round plume with initial velocity w_0. The material volume which is discharged from the source over a time interval Δt has a buoyancy force which is equal to the rate of change of the vertical momentum of the plume element,

$$\frac{dM}{dt} = F. \tag{2.58}$$

Assuming constant F, a simple integration of the above equation gives

$$M = M_0 + Ft \tag{2.59}$$

where M_0 and F are initial momentum and buoyancy fluxes respectively.
It is apparent that when there is a density differences, then there is a buoyancy force which generate fluid motion. According to spreading hypothesis, the plume spreads linearly with height, $\frac{db}{dz} = \beta$. From the chain rule

$$\frac{db}{dt} = \frac{db}{dz}\frac{dz}{dt} = \beta\overline{w} \tag{2.60}$$

By using Equation 2.33 and 2.59 together with the assumption of zero initial momentum, $M_0 = 0$, we will have

$$\overline{w} = \left(\frac{2Ft}{\pi}\right)^{\frac{1}{2}}\left(\frac{1}{b}\right) \tag{2.61}$$

Substituting the above equation into Equation 2.60, we will get

$$\frac{d}{dt}(b^2) = \beta\left(\frac{2Ft}{\pi}\right)^{\frac{1}{2}}. \tag{2.62}$$

After integrating both sides

$$b = \left(\frac{4\beta}{3}\sqrt{\frac{F}{\pi}t^3}\right)^{\frac{1}{2}}. \tag{2.63}$$

Substituting the value of b into Equation2.61 we get

$$\overline{w} = \left(\frac{3}{4\beta}\sqrt{\frac{F}{\pi t}}\right)^{\frac{1}{2}} \tag{2.64}$$

From the fact that $z = \frac{b}{\beta}$, the relationship between z and t can then be obtained as:

$$z = \left(\frac{4}{3\beta}\sqrt{\frac{F}{\pi}t^3}\right)^{\frac{1}{2}} \tag{2.65}$$

The expression for the volume, $Q = \pi b^2\overline{w}$ and momentum, $M = Ft$, fluxes is then given by

$$Q = \left(\frac{4\beta}{3}\sqrt{\pi F^3 t^5}\right)^{1/2} \tag{2.66}$$

$$M = \pi^{1/3}\left(\frac{3\beta F}{4}\right)^{2/3}\left(\frac{2F^{1/4}t^{3/4}}{3^{1/2}\pi^{1/4}\beta^{1/2}}\right)^{4/3} \tag{2.67}$$

2.5 Basic modeling assumptions

The assumptions made in the the analysis and mathematical modeling of this thesis report is listed below.

- Boussinesq approximation is used as the density difference is very small when compared with the reference density
- The plume is not in cross flow or coflow. The ambient fluid is assumed stagnant, linearly stratified and at rest which makes it non turbulent
- Spreading current is axis symmetric since the fluid is assumed in stagnant environment, a single exit pipe is considered.
- The heat exchange between the plume and the ambient water is ignored.

2.6 Initial conditions

Choosing an acceptable set of initial conditions will help us to review our mathematical models properly. It is a common phenomenon that the source of a plume might show a different plume characteristics. But the plume produced by the continuous source of buoyancy is likely to show a plume feature at a distance far from the source regardless of the source characteristics. For instance if we take the momentum flux of Equation 2.56, the initial momentum can not be zero. Hence, an appropriate values of initial conditions are very important to solve the ordinary differential equations. Let's denote b_0, w_{m0} and g'_0 are the initial conditions in the top-hat model. Then, the initial conditions for the volume, momentum and buoyancy fluxes become

$$Q_0 = b_0^2 w_{m0}, M_0 = b_0^2 w_{m0}^2, F_0 = b_0^2 w_{m0} g' \tag{2.68}$$

2.7 Sensitivity analysis of the plume

By considering a point source plume, we can choose the initial boundary conditions as $Q = 0$, $M = 0$, $F = F_0$ at $z = 0$. By dividing both sides of Equation 2.56 with $\frac{dF}{dz}$, we get

$$M\frac{dM}{dF} = -\frac{1}{N^2}F. \tag{2.69}$$

Integrating the above equation, assuming constant N, i.e linear stratification and given the boundary conditions, we obtain

$$M = \frac{1}{N}(F_0^2 - F^2)^{1/2} \tag{2.70}$$

The above equation shows that in linearly stratified environment the maximum buoyancy flux for a plume happens at the source, then it decreases with height. The notion of numerical sensitivity is that small change in the initial conditions must evoke only small change on the output. Lets assume for a point source plume rising in a linearly stratified environment, let's choose the initial conditions as

$$Q = M = F = 1 at z = 0. \tag{2.71}$$

According to Turner (1979) a pure point source plume with constant buoyancy frequency N, rises a finite height H_m by

$$H_m = 2.57 H_c \tag{2.72}$$

where

$$H_c = F_0^{1/4}(2\alpha)^{-1/2}N^{-3/4}. \tag{2.73}$$

Non-dimensionalization using H_c, the characterstics length and the source buoyancy flux F_0 is denoted as (Caulfield and Woods, 1998):

$$\frac{d\hat{Q}}{d\hat{z}} = \hat{M}^{1/2}, \quad \frac{d\hat{M}}{d\hat{z}} = \frac{\hat{F}\hat{Q}}{\hat{M}}, \quad \frac{d\hat{F}}{d\hat{z}} = -\hat{Q}\hat{N}^2. \tag{2.74}$$

where

$$\hat{Q} = \frac{Q}{(2\alpha)^{4/3}F_0^{1/3}H_c^{5/3}}, \quad \hat{M} = \frac{M}{(2\alpha)^{2/3}F_0^{2/3}H_c^{4/3}}, \quad \hat{F} = \frac{F}{F_0}, \quad \hat{N} = N \tag{2.75}$$

The non-trivial initial condition for the governing equation considered as,

$$\hat{Q} = \hat{M} = \hat{F} = 1. \tag{2.76}$$

To study the stability of the solutions, it is possible to take the perturbed initial condition which is

$$(\hat{Q}, \hat{M}, \hat{F})_\delta = (1, 1, 1) + \delta(\bar{Q}, \bar{M}, \bar{F}) \tag{2.77}$$

where δ is very small value which is less than 1.

By linearizing the governing equations, $\bar{Q}, \bar{M}$ and $\bar{F}$ would satisfy the following relationships

$$\begin{pmatrix} \frac{d\bar{Q}}{dz} \\ \frac{d\bar{M}}{dz} \\ \frac{d\bar{F}}{dz} \end{pmatrix} = \begin{pmatrix} 0 & 2\alpha & 0 \\ 0 & 0 & 1 \\ -N^2 & 0 & 0 \end{pmatrix} \begin{pmatrix} \bar{Q} \\ \bar{M} \\ \bar{F} \end{pmatrix} \tag{2.78}$$

Sensitivity analysis plays a fundamental role in mathematical modeling, engineering and statistics for broad ranges of applications. According to Saltelli et al. (2008) sensitivity analysis is the study of how the output of certain model is affected by the input parameters. According to Equations 2.55 - 2.57, the parameters which are found in the governing equations are α which is the entrainment constant and the square of the buoyancy frequency, N^2 . To achieve this, we need to calculate the rate of change of volume, momentum and buoyancy fluxes with respect to small perturbations in the input parameters. In the next part, we will do the derivation of the sensitivity equation for the governing equations below.

$$\frac{dQ}{dz} = 2\alpha M^{1/2} \tag{2.79}$$

$$\frac{dM}{dz} = F\frac{Q}{M} \tag{2.80}$$

$$\frac{dF}{dz} = -QN^2(z) \tag{2.81}$$

The first order sensitivity equation for the model parameter p_i, is defined as the vector $s_i = (s_1, ..., s_n)$

$$s_i(z, p) = \frac{\partial}{\partial p_i}(y(z, p)) \tag{2.82}$$

where n is the number of parameters, y is the ODE variable of the volume, momentum and buoyancy fluxes.

By using chain rule and simple differentiation, the derivative of the above equation is

$$s_i' = \frac{\partial f}{\partial y}s_i + \frac{\partial f}{\partial p} \tag{2.83}$$

$$s_i(z_0) = \frac{\partial z_0(p)}{\partial p_i} \tag{2.84}$$

where y,variables of the fluxes defined as

$$y'(z,p) = f(z, y(z); p) \tag{2.85}$$

$$y(z_0) = y_0 \tag{2.86}$$

In order to drive the sensitivities equations, we solve Equation 2.79 - 2.81 together with Equation 2.83 - 2.86. Thus, the sensitivities equation is given by (It is a scenario where the effect of the entrainment coefficient investigated by keeping the buoyancy frequency constant).

$$\frac{dQ}{dz} = 2\alpha M^{1/2} \tag{2.87}$$

$$\frac{dM}{dz} = F\frac{Q}{M} \tag{2.88}$$

$$\frac{dF}{dz} = -QN^2(z) \tag{2.89}$$

$$\frac{ds_1}{dz} = \frac{\alpha}{M^{1/2}}s_2 + 2M^{1/2} \tag{2.90}$$

$$\frac{ds_2}{dz} = \frac{F}{M}s_1 - \frac{QF}{M^2}s_2 + \frac{Q}{M}s_3 \tag{2.91}$$

$$\frac{ds_3}{dz} = -N^2(z)s_1 \tag{2.92}$$

with initial conditions of the sensitivities equations

$$s_1(0) = s_2(0) = s_3(0) = 0 \tag{2.93}$$

By using the above equations, the sensitivity of the buoyancy and momentum flux towards the entrainment constant has been computed and shown in Figure 2.5 and 2.6. The figures compare before and after the sensitivity analysis has been done and it shows the effect on the final rise height that is inline with the expected result.

The relative sensitivity equation of the plume model with respect to the buoyancy frequency can be obtained in a similar way like the previous equation. But in this case, we keep the entrainment coefficient constant.

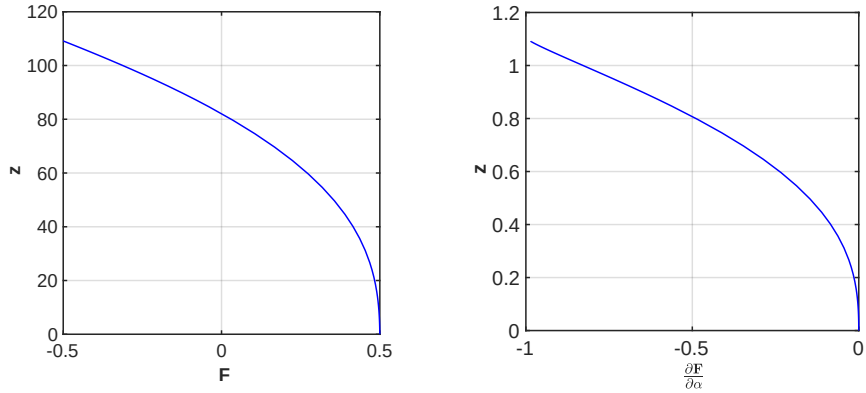

(a) Buoyancy flux with respect to depth.

(b) Sensitivity of buoyancy flux with respect to entrainment constant α.

Figure 2.5: Comparison of the buoyancy flux with it's sensitivity function with respect to the entrainment constant α . It is evaluated with initial values $(Q_0, M_0, F_0) = (0.1, 0.01, 1)$ with $\alpha = 0.0116$

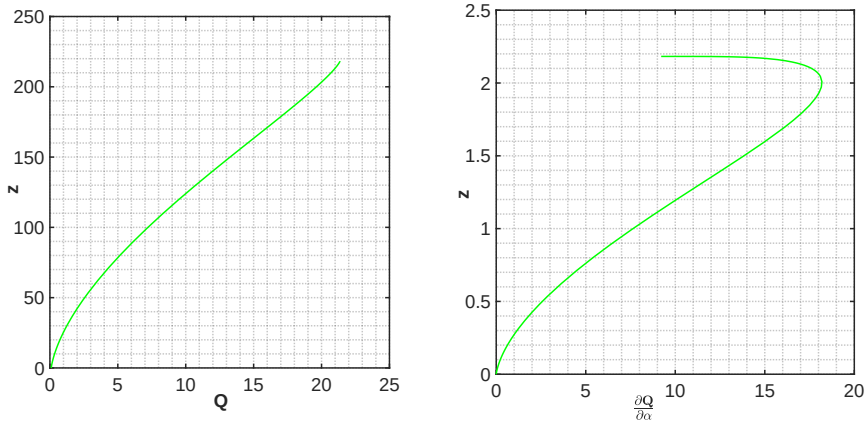

(a) Volume flux with respect to depth.

(b) Sensitivity of volume flux with respect to entrainment constant α.

Figure 2.6: Comparison of the volume flux with it's sensitivity function with respect to the entrainment constant α . It is evaluated with initial values $(Q_0, M_0, F_0) = (0.1, 0.01, 1)$ with $\alpha = 0.0116$

Thus, the sensitivity equations for the integral model are:

$$\frac{dQ}{dz} = 2\alpha M^{1/2} \tag{2.94}$$

$$\frac{dM}{dz} = F\frac{Q}{M} \tag{2.95}$$

$$\frac{dF}{dz} = -QN^2(z) \tag{2.96}$$

$$\frac{ds_1}{dz} = \frac{\alpha}{M^{1/2}}s_2 \tag{2.97}$$

$$\frac{ds_2}{dz} = \frac{F}{M}s_1 - \frac{QF}{M^2}s_2 + \frac{Q}{M}s_3 \tag{2.98}$$

$$\frac{ds_3}{dz} = -N^2(z)s_3 - Q \tag{2.99}$$

with initial conditions

$$s_1(0) = s_2(0) = s_3(0) = 0 \tag{2.100}$$

The results in Figure 2.7 and 2.8 shows the plume model predicts the sensitivity of the volume flux towards the buoyancy frequency by an average factor of 10^{-2}. This value is approximately consistent within the data that shows the density variation of the environment.

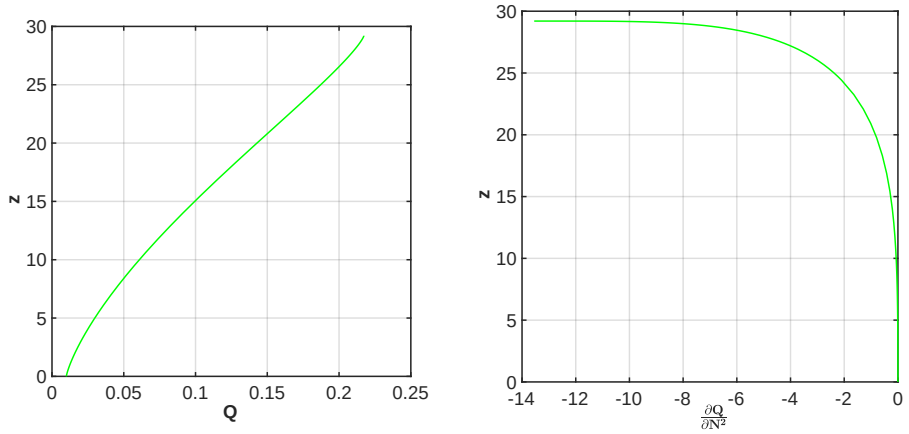

(a) Volume flux

(b) Sensitivity of volume flux to entrainment constant α

Figure 2.7: Comparison of the volume flux with it's sensitivity function with respect to the buoyancy frequency N^2 . It is evaluated with initial values $(Q_0, M_0, F_0) = (0.1, 0.01, 1)$ with $\alpha = 0.0116$

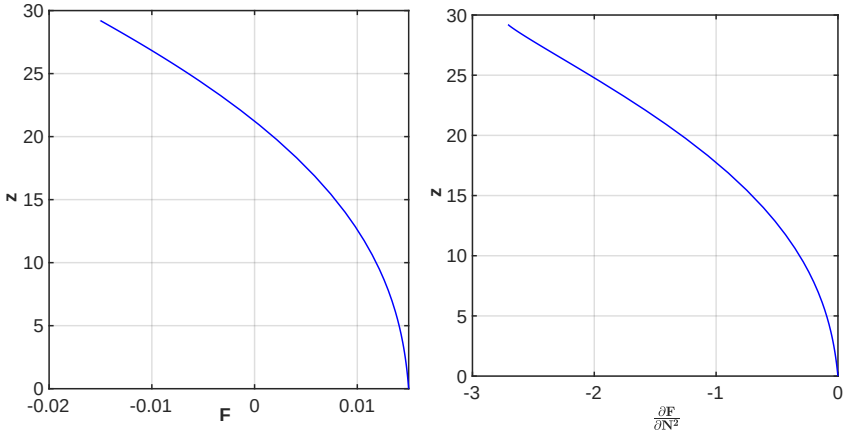

(a) Buoyancy flux

(b) Sensitivity of buoyancy flux to buoyancy frequency N^2.

Figure 2.8: Comparison of the buoyancy flux with it's sensitivity function to the buoyancy frequency N^2 . It is evaluated with initial values $(Q_0, M_0, F_0) = (0.1, 0.01, 1)$ and $\alpha = 0.0116$

2.8 Numerical model setup and results

The numerical model analysis of the plume is based up on the basic governing equations which was discussed in Section 2.1.1. In addition the sensitivity of the model with regards to the variation of certain variables has also been tested. The plume is expected to have initial momentum at the source, however we assumed that it's influence is mainly confined around the source. As it has been discussed in the previous sections, we follow axis symmetric fresh water submerged vertical plume in a uniformly stratified environment.

The mathematical model which was written using Matlab ODE 45 has two major parts. The first test case which uses source radius, vertical velocity and reduced gravity; assesses the general entrainmnet models which was set by Morton et al. (1956). Different maximum height predictions has also been discussed. In the second part, the same analysis is performed but the plume model has run using volume, momentum and buoyancy fluxes.

Table 2.1 shows test cases for a discharge with a round source of 2m diameter. In each test cases, the same initial reduced gravity is used. Table 2.1 summarizes the initial parameters involved in all of the four tests. In all of the tests, the plume rises up to the neutral buoyancy level where the buoyancy flux becomes zero as the density difference between the plume and its surrounding decreases to zero. Then the plume overshoots the neutral buoyancy level due to inertia. It then falls back because of the negative buoyancy and spreads out horizontally as a level of equilibrium.

Test	Pipe diameter (m)	Discharge $(m^3 s^{-1})$	Initial vertical velocity (ms^{-1})	Initial reduced gravity (ms^{-2})
1	2	$3.14 * 10^{-2}$	0.01	1
2	2	$15.7 * 10^{-2}$	0.05	1
3	2	$31.4 * 10^{-2}$	0.1	1
4	2	$62.8 * 10^{-2}$	0.2	1
5	1	$7.85 * 10^{-2}$	0.1	1
6	2	$31.4 * 10^{-2}$	0.1	1
7	3	$70.65 * 10^{-2}$	0.1	1
8	4	$125.6 * 10^{-2}$	0.1	1

Table 2.1: Initial values used in execution of the plume model

Figure 2.9 shows the mean vertical velocity along the depth where finally hits a maximum height, z_m and becomes zero. The tests from 5 to 8 in Table 2.1 show that a larger outlet diameter is required to entrain large amount of ambient fluids to the required depth.

The test results in Table 2.2 shows the same amount of discharge for different pipe diameters with the same initial buoyancy fluxes. According to Equation 1.1, the plume formed is classified as a lazy plume. When we look at the initial conditions, we might presume different plume characteristics. Test 1 has $1m$ while test 4 has $4m$ pipe diameter (from Table 2.2). One can expect that all test cases from Table 2.2 could show different plume characteristics. However the results show the opposite. For instance, the result in Figure 2.12 shows that the difference is very small in all cases which implies the plume shows similar characteristics regardless of the initial conditions which has a considerable source diameter difference.

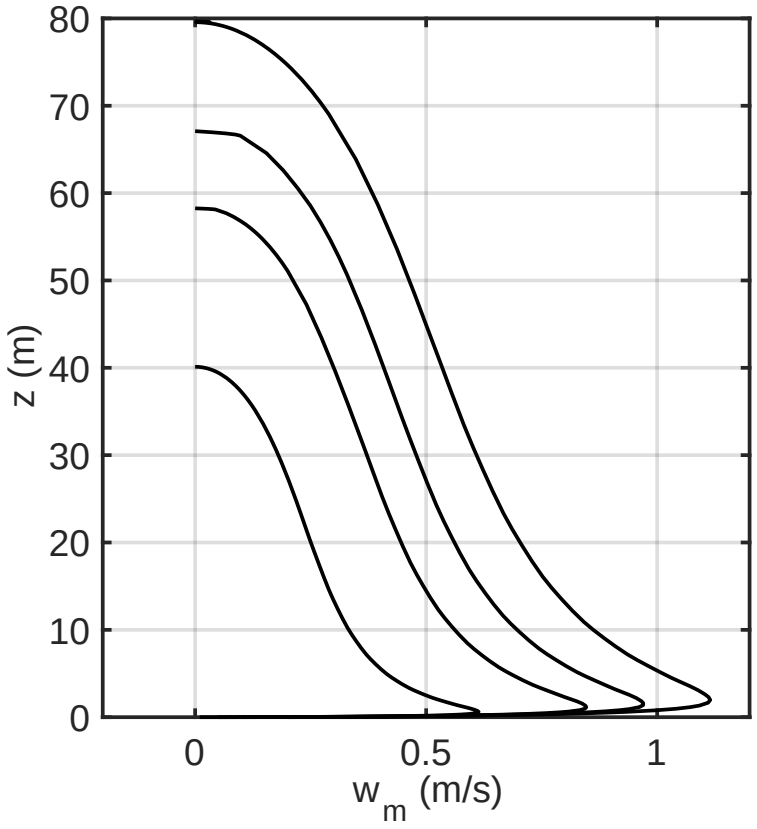

Figure 2.9: Mean vertical velocity along with depth with different initial velocities.

The vertical velocity trajectory for a different pipe diameter is shown in Figure 2.10. The data is taken from Table 2.2. The result shows for the given discharge, the larger exit diameter gives a higher rise height .According to Equation 3.21, the length scale defined as $\frac{M_0^{3/4}}{F_0^{1/2}}$ has a maximum value of ≈ 0.09. This is a distance where momentum would become negligible and the dominant effect is only the force of buoyancy.

Test	Discharge $(m^3 s^{-1})$	Initial Momentum Flux $(m^4 s^{-2})$	Initial Buoyancy Flux $(m^4 s^{-3})$	Pipe diameter (m)
1	$7.85 * 10^{-2}$	$0.785 * 10^{-2}$	$7.85 * 10^{-2}$	1
2	$7.85 * 10^{-2}$	$0.196 * 10^{-2}$	$7.85 * 10^{-2}$	2
3	$7.85 * 10^{-2}$	$0.085 * 10^{-2}$	$7.77 * 10^{-2}$	3
4	$7.85 * 10^{-2}$	$0.049 * 10^{-2}$	$7.85 * 10^{-2}$	4

Table 2.2: Initial values of parameters of similar discharge

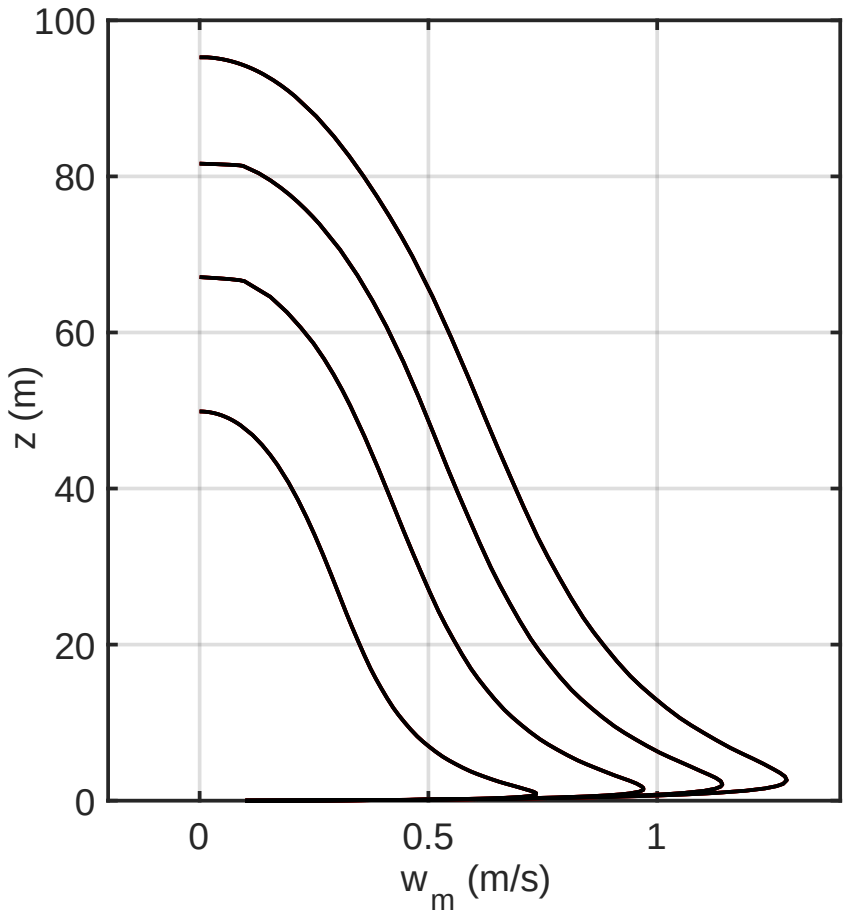

Figure 2.10: Mean vertical velocity along with depth with different discharge outlet diameters.

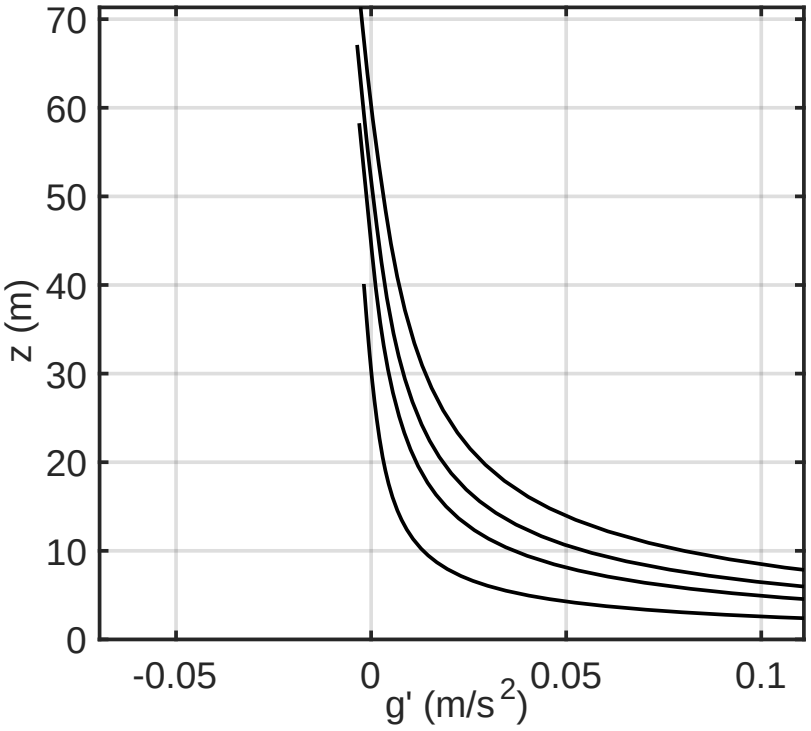

Figure 2.11: Reduced gravity plot along the plume axis for different initial velocities. In all cases initial reduced gravity and source diameter are the same. NB: The figure is zoomed in.

Figure 2.11 shows that the density variation profile for different initial velocities along the trajectory of the plume. The data is taken from test 1 to 4 of Table 2.1. From the figure we can see that the depth where the density of the rising plume equal to the ambient density and the depth where the plume reaches maximum height. For these initial conditions, the maximum height is expected to be few meters distance above the equilibrium point. We can see that as the discharge increases, it's rise height increases but the plume entrains smaller amount of fluid.

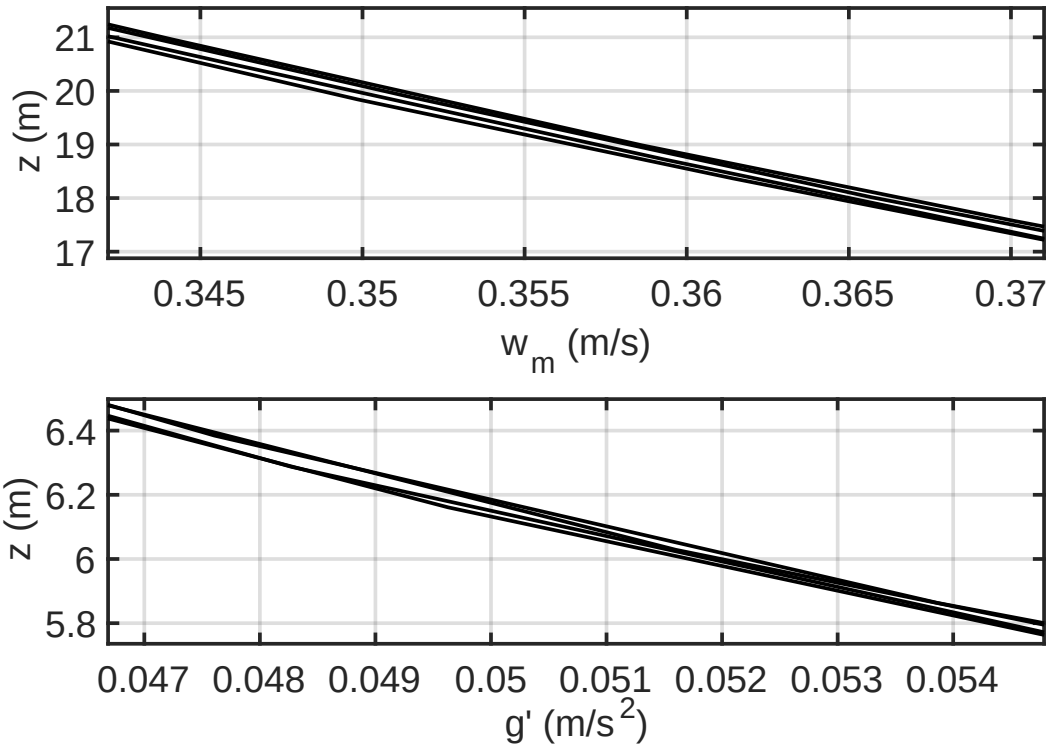

Figure 2.12: Vertical velocity and reduced gravity. Both figures have the same initial discharges but different pipe diameters. Despite the significant pipe diameter difference, both figures have similar plume characteristics.

The final volume flux is the sum of the upward volume flux at the level of neutral buoyancy and the downward volume flux at the maximum height. The numerical experiment data of Devenish et al. (2010) show that this flux comprise 80% and 19% of the final volume flux respectively. This strongly supports the assumption made by Devenish et al. (2010) that for a rising plume, the plume top and the overlapping region are the main area of entrainment. In many cases, the source flux conditions are unknown far from the source but it is not difficult to observe the maximum plume height. The relationship between z_{max} and F_0 is presented in Section 3.3. Rooney and Devenish (2014) has provided a relationship between z_{max} and final volume flux, Q by eliminating F_0 , as:

$$z_{max} = 1.34\pi^{-1/3}\alpha^{-2/3}N^{-1/3}Q^{1/3} \tag{2.101}$$

In a similar fashion, Bursik et al. (1992) come up with the formula for the relationship between z_{max} and final volume flux, Q as

$$z_{max} = 22\pi^{-1/3}\alpha^{-2/3}N^{-1/3}Q^{5/26}. \tag{2.102}$$

The coefficient and exponent are clearly seen different in Equation 2.102. Though both of the equations give similar results for specific height range as described in Rooney and Devenish (2014), the result from thesis's data, as shown in Figure 2.13, shows a significant difference among them. But it is not uncommon to have this level of difference between Equation 2.101 and 2.102. Some data on which mathematical models are based might have an error in logarithmic scale (Sparks, 1986).

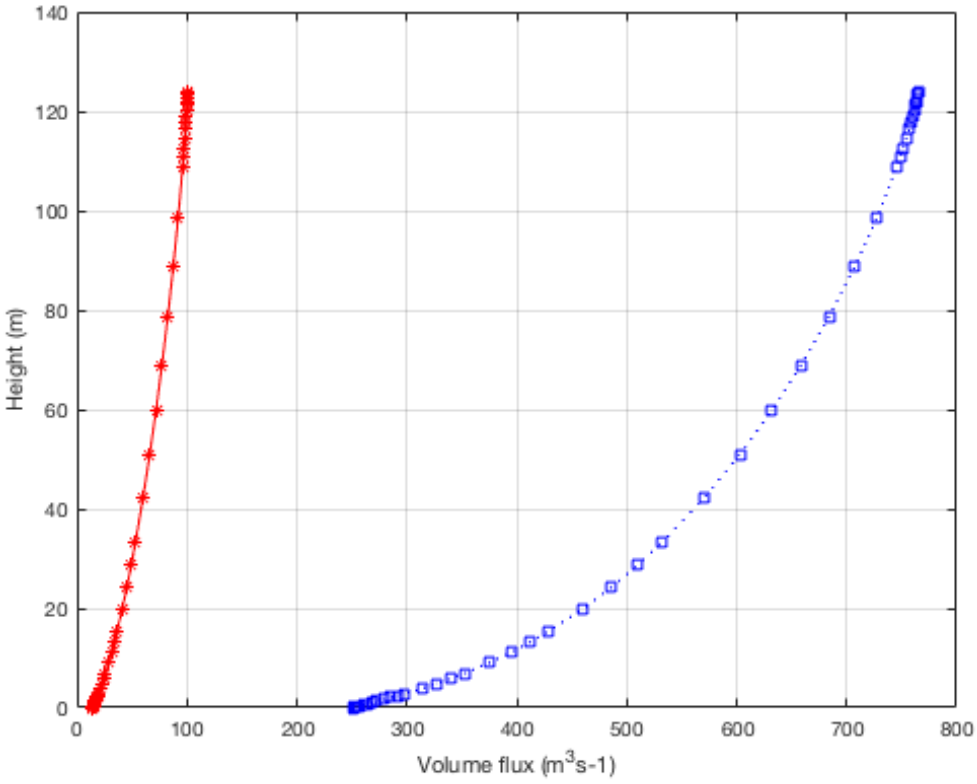

Figure 2.13: Final plume volume flux as a function of maximum height. The graph in red dot line represent the relationship in Equation 2.101 and the graph in blue dot represent the relationship in Equation 2.102

The result in Figure 2.14 shows the width of the plume increases with distance from the source. The spreading rate of around 0.17 is observed from this result. It appears that this result is inline with the experimental results of the spreading

rate variation from $\beta = 0.102 \approx 0.114$ Lee and Chu (2003). The spreading rate for the concentration profile is different from the rate for the velocity profile. The characteristics radius of the concentration profile is the ratio of the concentration to the velocity width; $\lambda = \frac{b_c}{b_v}$.

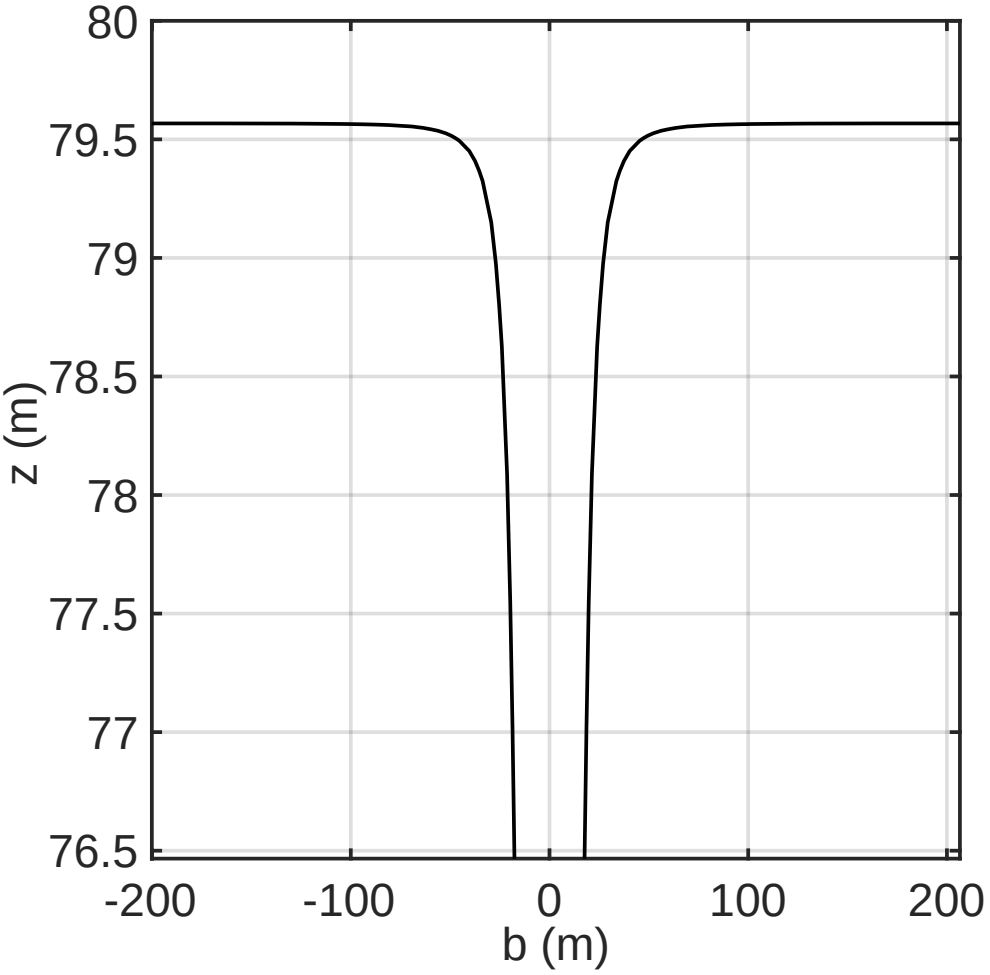

Figure 2.14: Plume width as a function of height. The figure is zoomed in.

For most practical reasons, a constant spreading rate of $\beta = \frac{db_v}{dz} \approxeq 0.108$ may be applied for both jets and plumes Lee and Chu (2003). Because of the scope of this thesis, we haven't covered the concentration profile analysis.

Chapter 3

Results and analysis

3.1 Data analysis in different scenario

In this chapter we are going to analyze and obtain estimates of a plume formation in stagnant environment for a different scenario. It also covers the maximum height obtained by the plume and also analyses the effects of initial conditions. All the formulations and assumptions are based up on those described on the previous chapters.

3.1.1 Uniform environment

A uniform environment is of uniform density where $N = 0$. Integrating the buoyancy flux in Equation 2.39 gives out a constant buoyancy flux,

$$b^2 w_m g' = F_0, \tag{3.1}$$

where F_0 is the initial buoyancy flux. Thus, it shows that the buoyancy flux remains positive and constant with a height in a uniform environment. Then the corresponding integral equation become

$$\frac{d(b^2 w_m)}{dz} = 2\alpha b \tag{3.2}$$

$$\frac{d(b^2 w_m^2)}{dz} = b^2 g' \tag{3.3}$$

$$\frac{d(b^2 w_m g')}{dz} = 0 \tag{3.4}$$

The far-field solution to the above integral equation is proposed by Morton et al. (1956) by assuming asymptotic solution where $b(z) = a_b z^{n_b}$, $w(z) = a_w z^{n_w}$ and

$g'(z) = a_g z^{n_g}$. By equating coefficients that has equal power of z, we get

$$b = \frac{6}{5}\alpha z, \tag{3.5}$$

$$w_m = \frac{5}{6\alpha}\left(\frac{9}{10}\alpha F_0\right)^{1/3} z^{-1/3}, \tag{3.6}$$

$$g' = \frac{5}{6}\frac{F}{\alpha}\left(\frac{9}{10}\alpha F\right)^{-1/3} z^{-5/3}. \tag{3.7}$$

It can be seen that as z approaches the source, w_m and g' goes to ∞ that shows a mathematical singularity where we can not able to predict in this condition. One way to avoid this problem is to have a virtual source location where the initial volume and momentum flux is different from zero so that the system will be well posed (Tzou, 2015). The different ways of determining the location of the virtual source where it matches the initial conditions, is presented in Hunt and Kaye (2001). By employing the same mechanism in finding the asymptotic solution of the above integral equation, the solution for the volume, momentum and buoyancy flux become

$$Q = \frac{6\alpha}{5}2^3\left(\frac{9}{10}\alpha F\right)^{1/3} z^{5/3} \tag{3.8}$$

$$M = 2^{1/3}\left(\frac{9}{10}\alpha F\right)^{2/3} z^{4/3} \tag{3.9}$$

$$F = F_0 \tag{3.10}$$

As formulated theoretically, in a uniform environment the plume goes up to the surface as long as it is less dense than the environment. Figure 3.1a shows increasing the buoyancy flux drives much water to the surface. But if we keep the buoyancy flux constant, the volume flux exhibits no change at all no matter how we vary the initial momentum and volume flux. In the same way it has shown in Figure 3.1b and 3.1c that even if we increase the discharge, the plume wouldn't entrain the surrounding fluid to the needed depth. However the volume flux that reaches the surface increases as the discharge increases. Notice that in the presence of friction and wave effects, the distance traveled by the plume reduces significantly due to the friction takes out of the energy. In this thesis, those effects are neglected.

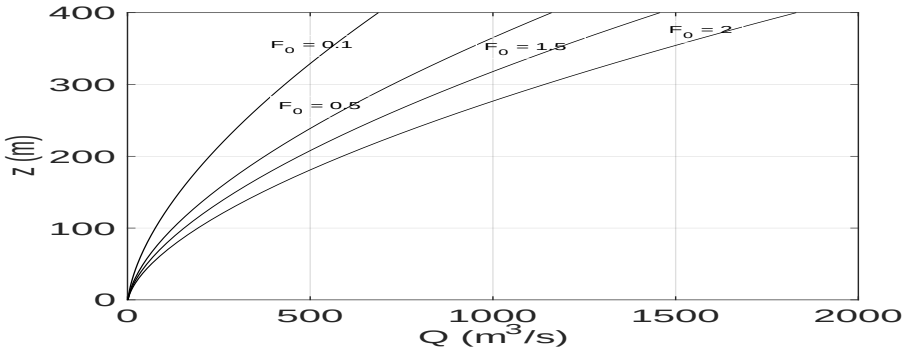

(a) Constant initial volume and momentum fluxes which is, $Q_0 = 1.5\,m^3/s$ and $M_0 = 0.5\,m^4/s^2$ in all of the simulations. Buoyancy flux, $F_0 = 0.1,\ 0.5,\ 1$ and $2\,m^4/s^3$.

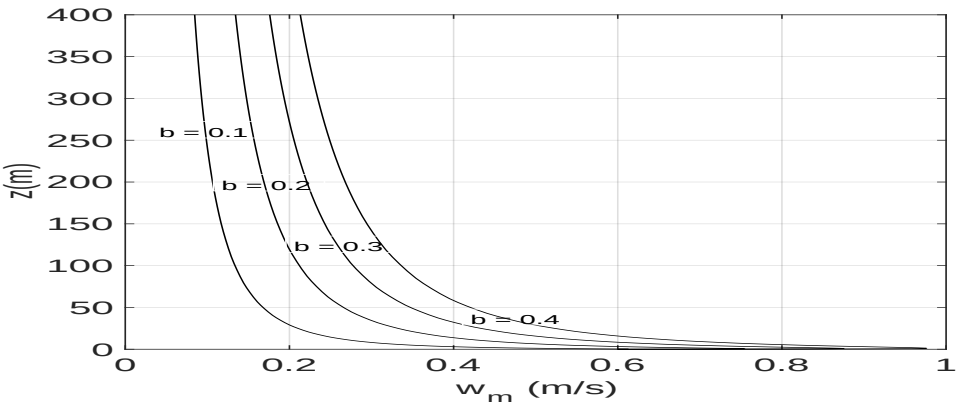

(b) Constant exit velocity $w = 0.6\,m/s$ and reduced gravity $g' = 1\,m/s^2$ in all cases. Exit radius $b = 0.1,\ 0.2,\ 0.3$ and $0.4\,m$.

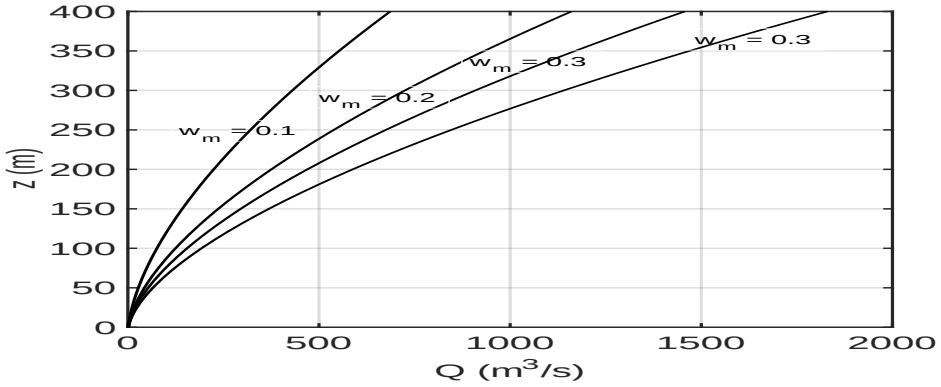

(c) Constant exit diameter $D = 1.2\,m$ and initial reduced gravity $g' = 1\,m/s^2$ in all cases. Initial exit velocity $w_m = 0.1,\ 0.2,\ 0.3$ and $0.4\,m/s$

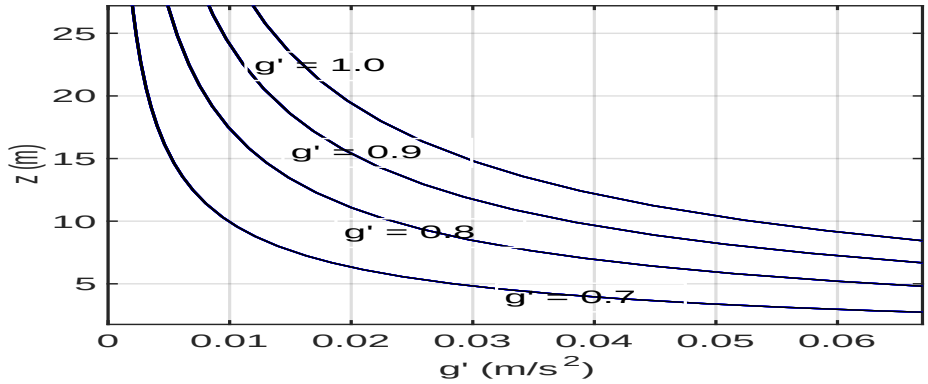

(d) Constant exit diameter $D = 0.8\,m$ and initial vertical velocity $w_m = 0.6\,m/s$ in all cases. Initial reduced gravity $g' = 0.7$, 0.8, 0.39 and $1.0\,m/s^2$

Figure 3.1: The numerical solution for maximum rise height achieved by the plume compared with the rise height formula presented by Briggs (1970) in Equation 3.30

.

3.1.2 In linearly stratified environment

In general, uniform stratification occurs often in oceans and atmospheres. In the ocean it is determined by the physical water properties such as salinity and temperature. The density of sea water increases with increasing salinity and decreases with increasing temperature. In stable conditions, the least dense water lies on top of heavier water layer. In most cases, this water layers are stably stratified. The situation such as low saline water on top of a high saltier deep water is a very common phenomenon which is found in fjords and around it's coastal areas which gets runoff fresh waters from streams and rivers (Golmen, 1998). Figure 3.2 shows an example of how salinity, temperature and density varies with depth in fjords.

As it was discussed in Section 2.1.3, the movement of the fluid element that moved downward tends to return to it's equilibrium position since it would become lighter. This oscillation is called local buoyancy frequency (Turner, 1979).

$$N(z) = \sqrt{-\frac{g}{\rho_0}\frac{d\rho_a}{dz}} \tag{3.11}$$

The stratification can be said stably stratified if $\frac{d\rho_a}{dz} < 0$ and unstably stratified if $\frac{d\rho_a}{dz} > 0$ by assuming z is upward. According to the data in Appendix A.3, the value of $\frac{g}{\rho_0}\frac{d\rho_a}{dz}$ is in the order of 10^{-4} to 10^{-5} which is similar with the values found in

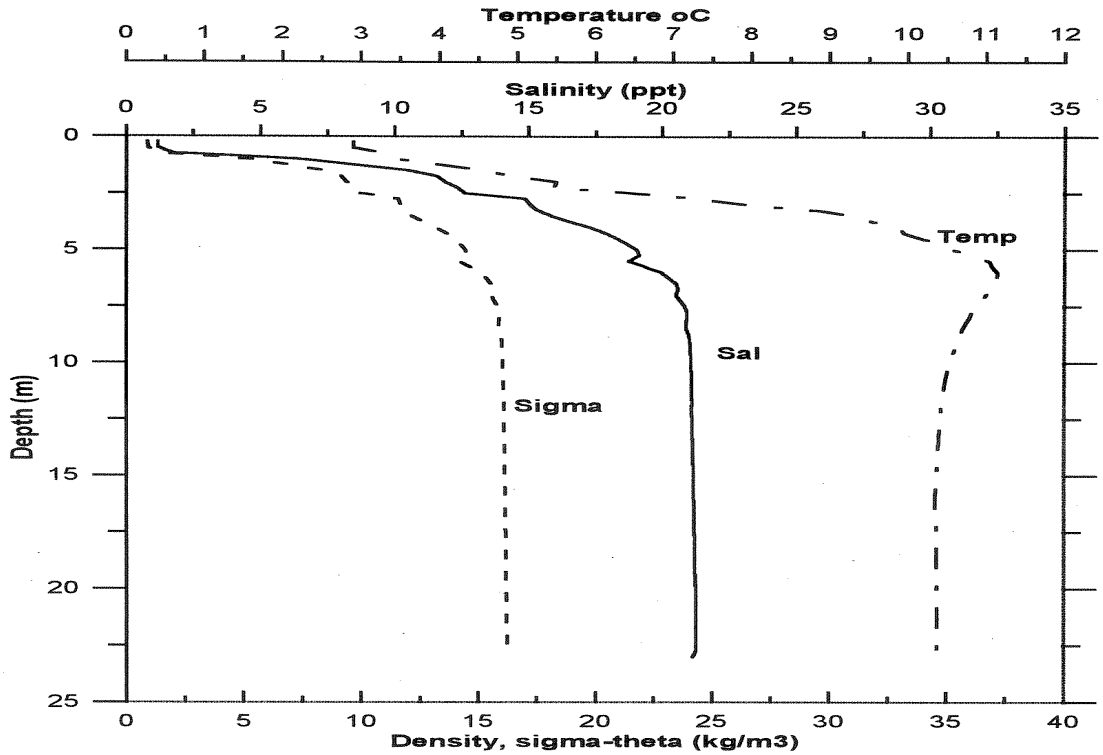

Figure 3.2: The diagram shows the interrelationship between salinity, density and temperature of the oceanic waters in fjords (Golmen, 1998)

lakes and oceans (Fischer et al., 1979). In non uniformly stratified environment, the displaced fluid moved downward would become lighter than it's environment, has a tendency to move towards it's equilibrium position (Lee and Chu, 2003).

3.2 Plume height and spreading scenario

Lagrangian method is generally an alternative approach in solving the maximum height reached by the plume. Due to momentum, at the neutral buoyancy level where the density difference between the plume and it's surrounding is zero, the plume overshoots. Upon reaching the maximum height where the momentum flux is zero, the plume falls back and spread out forming a horizontal layer.
From chain rule, we have $\frac{dF}{dt} = \frac{dF}{dz}\frac{dz}{dt}$. By using Equation 2.57 and $M = Q\overline{w}(z,t)$, the time derivative of the buoyancy flux become

$$\frac{dF}{dt} = -MN^2(z,t) \tag{3.12}$$

In the same way as above, we have $\frac{dM}{dt} = \frac{dM}{dz}\frac{dz}{dt}$. By using Equation 2.56, the momentum increase with time at a rate equal to the buoyancy flux:

$$\frac{dM}{dt} = F \tag{3.13}$$

By combining Equations 3.12 and 3.13, we get

$$\frac{d^2}{dt^2}M + MN^2 = 0 \tag{3.14}$$

It is a simple harmonic oscillator equation and the general solution with initial momentum M_0 is

$$M = A\cos Nt + B\sin Nt \tag{3.15}$$

where $A = M_0$ and $B = \frac{F_0}{N}$. By combining with equation of momentum, Equation 3.15 can be rewritten as

$$\pi b^2 w^2 = \frac{F_0}{N}\sin Nt + M_0\cos Nt \tag{3.16}$$

Since $\frac{dz}{dt} = w$ and $b = \beta z$, the above equation become

$$\frac{dz}{dt}\beta z = \frac{1}{\sqrt{\pi}}\left(\frac{F_0}{N}\sin Nt + M_0\cos Nt\right)^{1/2} \tag{3.17}$$

After some rearrangements and substitution, we get

$$z = \frac{\sqrt{2}}{\pi^{1/4}\beta^{1/2}}\int\left(\frac{F_0}{N}\sin Nt + M_0\cos Nt\right)^{1/4}. \tag{3.18}$$

The formula for height z of the plume penetration can be written as:

$$z = \frac{\sqrt{2}}{\pi^{1/4}\beta^{1/2}}(I(\tau))^{1/2} \tag{3.19}$$

where $\tau = Nt$ and $I(\tau) = \int_0^\tau \left(\sqrt{M_0 cos\tau' + \frac{F_0}{N} sin\tau'}\right)$.

The integral model in determining the entrainment process which was developed by Morton et al. (1956) breaks down shortly after the plume reaches the maximum height and starts to re-entrain the mixed fluid from the spreading layer. Wong and Wright (1988) showed a formula for the thickness of the spreading layer, h_e as

$$h_e = 1.7F_0N^{-3/4} \tag{3.20}$$

This implies that the spreading layer thickness may account for 38% of the total height in linearly stratified fluids. So it could be said with certainty that to use the integral method is improper.

The process of mixing and entraining of the fluid vary with the distance from the source. The near field which is a region in the neighborhood of the source where initial mixing takes place. The momentum and buoyancy at the source determines the flow pattern. In the near filed the plume acts like buoyant jets and then it converted to a pure plume far from the source. According to Lee and Chu (2003), the measure of a distance length scale defined by the buoyancy and momentum fluxes at which the behavior of the discharged jet exhibits plume like characteristics in stagnant environment, is given by

$$l_s = \frac{M_0^{3/4}}{F_0^{1/2}}. \tag{3.21}$$

After conducting a series of experiments, Papanicolaou and List (1988) come up with, for a certain distance from the source they defined a dimensionless distance, z/l_s from the flow source to attain asymptotic flows. The experiment involved the measurements of w, v and ρ at a different distance from the origin. The results of their experiments show that the flow behaves like a jet for $z/l_s < 1$ and like a plume for $z/l_s > 5$. For the value of z/l_s between 1 and 5, the flow transforms from jets to plumes.

3.3 Maximum height

For a plume, the initial momentum can be ignored far from the source. Then Equation 3.15 become

$$\pi b^2 w^2 = \frac{F_0}{N} \sin Nt \tag{3.22}$$

Since $\frac{dz}{dt} = w$ and $b = \beta z$, the above equation can be rewritten as:

$$\sqrt{\pi}\frac{dz}{dt}\beta z = \sqrt{\frac{F_0}{N}}(\sin Nt)^{1/2} \tag{3.23}$$

By integrating both sides, we can come up with:

$$z^2 = \frac{2}{\beta\sqrt{\pi}}\sqrt{\frac{F_0}{N}}\int_0^t \sqrt{\sin\ Nt}\, dt \tag{3.24}$$

The maximum height occurs at a point where the momentum flux goes to zero.

Hence $sin(Nt) = 0$, integrating Equation 3.24 from $t = 0$ to $t = \pi/N$ gives the maximum height the plume rises.

$$z_{max} = \frac{\sqrt{2}}{\sqrt{\beta}\pi^{1/4}}\left(\frac{F_0}{N}\right)^{1/4}\left(\int_0^{\pi/N}\sqrt{\sin Nt}\,dt\right)^{1/2} \tag{3.25}$$

This can be simplified as shown in Appendix B.1 and the final result become

$$z_{max} = \frac{\pi^{1/4}}{\sqrt{\beta}}F_0^{1/4}N^{-3/4} \tag{3.26}$$

By assuming the spreading constant, $\beta \approx 0.11$, we will have

$$z_{max} = 4.0\,F_0^{1/4}N^{-3/4} \tag{3.27}$$

After reaching the maximum height, the plume changes direction and starts to entrain the mixed fluid and the upward flow. At this point, the integral formulation cannot be used in determining the final height. According to experimental observations, the plume top fluctuates in steady state at a height about $0.7z_{max}$ Turner (1979). However, the spreading hypothesis has a reasonable solution which is obtained by Morton et al. (1956).

$$z_{max} = 4.02F_0^{1/4}N^{-3/4} \tag{3.28}$$

According to Lee and Chu (2003), the above equation can be rewritten using the entrainment hypothesis as:

$$z_{max} = 1.15\alpha^{-1/2}F_0^{1/4}N^{-3/4}. \tag{3.29}$$

Briggs (1970) has also come up with plume rise formula after doing laboratory experiments as:

$$z = 3.76\,F_0^{1/4}N^{-3/4}. \tag{3.30}$$

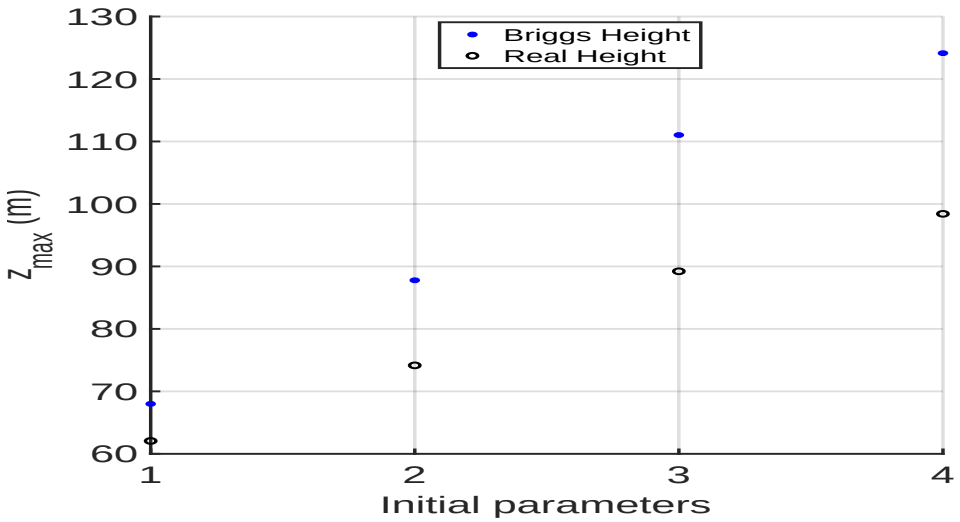

(a) Constant exit velocity w, and reduced gravity g' for each of the tests is $0.15\,m/s$ and $1\,m/s^2$ respectively. Exit radius for each of the four tests is $b = 0.6,\ 1,\ 1.6\,and\,2\,m$ respectively. The horizontal axis represents the tests for each initial value parameters consecutively.

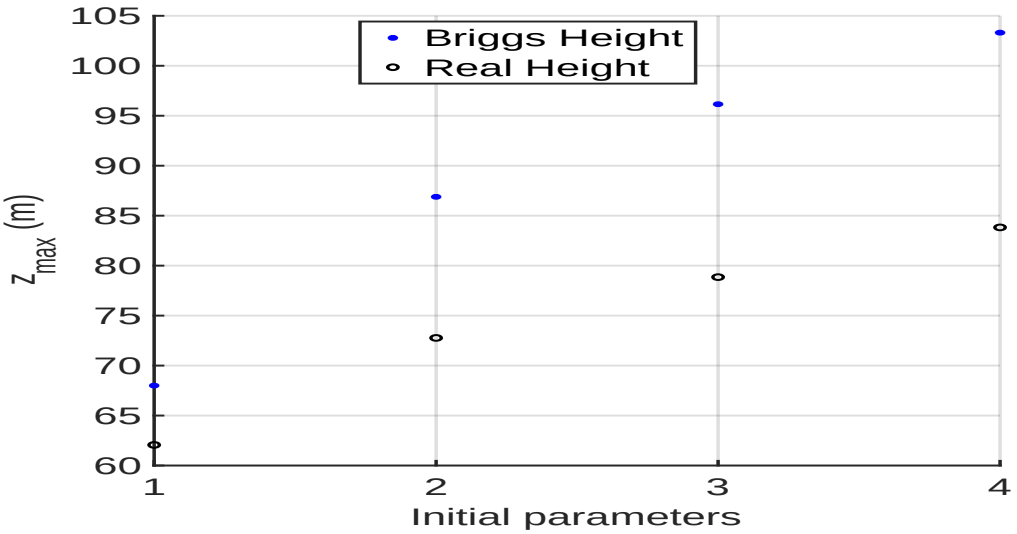

(b) Constant exit radius b, and reduced gravity g' for each of the tests is $0.6\,m$ and $1\,m/s^2$ respectively. Exit velocity for each of the four tests is $b = 0.15,\ 0.4,\ 0.6\,and\,2\,m/s$ respectively. The horizontal axis represents the tests for each initial value parameters consecutively.

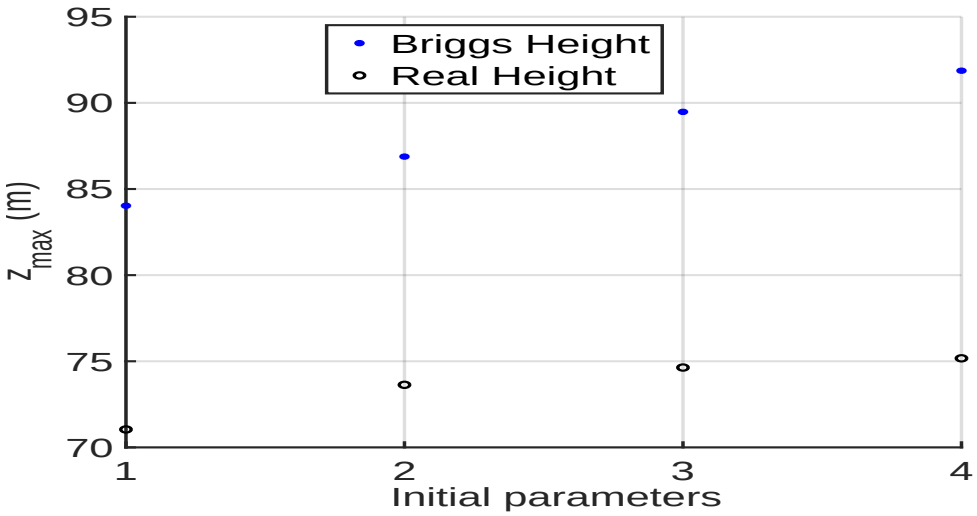

(c) Constant exit velocity w and radius $b, 0.5\,m/s$ and $0.6\,m$ respectively. Reduced gravity, $g' = 0.7, 0.8, 0.9, and\, 1\,m/s^2$. Constant exit velocity w, and source radius b' for each of the tests is $0.5\,m/s$ and $0.6\,m$ respectively. Reduced gravity, g' for each of the four tests is $g' = 0.7,\ 0.8,\ 0.9\, and\, 1\,m/s^2$ respectively. The horizontal axis represents the tests for each initial value parameters consecutively.

Figure 3.3: The numerical solution for maximum rise height achieved by the plume compared with the rise height formula presented by Briggs (1970) in Equation 3.30

As Figure 3.3 shows the predicted maximum plume height compared to the plume height prediction given by (Briggs, 1970) in Equation 3.30 which can be seen that is in the good agreement for the rise height. But we can observe from the result that as the initial values increases the gap between the two results also increases with certain amount. But when it comes to reduced gravity as in Figure 3.3c, the difference is considerable since stratification is a very important factor in affecting height depth. In general, increasing the exit velocity and diameter increases the height achieved by the plume.

3.4 Theoretical result of an entrainment coefficient

The entrainment model set by Morton et al. (1956) enables us for the description of the flow in a plume. Although a lot of work has been made in understanding the turbulent nature of a plume, the appropriate value of the entrainment coefficient is an

open question. Most of experimental evidences suggest that α is not a constant value. It can vary by as much as 60 percent over from jet to plume range, from $\alpha_{jet} = 0.057$ for the round jet to $\alpha_p \approx 0.09$ for the round plume. To obtain a numerical prediction of this entrainment constant, we have used a method of parameter estimation of a differential equation in ODE 45. By using the value of the square of the buoyancy frequency N^2 fixed at $N^2 = 10^{-2}$, the value of α varied between $1*10^{-2}$ to $11.6*10^{-2}$. These values of α_p is used in calculating the rise height in Equation 2.101 and Equation 2.102. The numerical prediction of an entrainment constant of $\alpha = 0.025$ is found that agrees significantly well with the experimentally determined value of α.

Chapter 4

Summary, Conclusion and future Work

4.1 Summary and conclusion

This thesis has presented a mathematical model formulations for the prediction of spreading and rising of a round buoyant fresh water plume in uniformly stratified and stagnant environments. Specifically, we have examined the case of fjords. The study outlined the preliminary understanding of buoyant plume behavior based on plume conservation equation and its closure entrainment assumption model. The entrainment equation is used to quantify the turbulent mixing between the flow and the environment. Mathematical modeling has been carried out to predict the maximum and spreading heights among with the width, height, velocity, buoyancy, mass and momentum all over to the top of the plume. The mathematical model equation is based on the plume vertical gradient of the volume, momentum and buoyancy fluxes.

The physical flow process of a submerged fresh water plume is divided into two zones: Zone of flow establishment (ZFE) and Zone of established flow (ZEF). The connection between the top-hat and Gaussian profiles with ZFE and ZEF is presented in Chapter 2. In many cases the usual discharge possess both momentum and buoyancy. In the previous chapters, we have looked at jet behavior is governed by momentum while plume behavior is governed by buoyancy. For a source directed vertically upward, the kinetic energy of the motion decreases with height. At certain point, the effects of buoyancy dominate. For positively buoyant plume, the buoyancy acts in the same direction as the transport flow and it serves to increase the momentum flux.

The numerical results presented in Chapter 2 using the source and ambient conditions show that it is possible to raise a significant amount of sea water to any

distance from the source by using fresh water plume. The maximum penetration height of the plume by using Lagrangian method was developed. It is based on the volume due to release of buoyancy at the source of the plume over a period of a time unit. The result predicts that the volume flux decreases to zero at the maximum height, indicating further mixing and re-entrainment as the plume fluid falls back. The numerical results also indicate that the time taken for the volume flux to reach a maximum height is independent of the buoyancy flux. Still this time, the exact value of α is not defined precisely. The value taken from experimental measurements vary considerably. Morton (959b) have found a value of 0.116 for top hat profiles for plumes. In this thesis, numerical prediction of α has been made by using the method of parameter estimation and the result agrees well significantly with the expermentally determined value of α.

When the vertical distance from the source is not significantly larger than the plume width, the entrainment model is unlikely to be valid. Recent studies indicate the different entrainment coefficient models are mostly for fully developed flows and in some areas such as the region of transition from forced to pure plume (Bhamidipati and Woods, 2017). In the end a theoretical model is developed to examine the sensitivity of the plume model to a conditions the entrainment constant and buoyancy frequency. It highlights how sensitive is the plume model with respect to the input parameters.

4.2 Future work

This thesis work has examined the analysis of vertical plume that has provided the basic understanding of turbulence and mixing in plumes with some mathematical models in obtaining consistent estimates of results. However in some engineering applications, there might be a need to place the source at a vertical or horizontal angle of discharge. The possible future extension of this thesis could include a model for the case of an inclined plumes.

A single point discharge is assumed in this thesis work. But practical application requires extension of this to multiport diffusers. Analyzing the orientation of the plume flow with respect to the ocean currents can also be important. Furthermore, in any multiple point discharges, the individual plumes merges to form clusters of plumes flow. All of this feature create combinations of plume flow and interactions between the plume which can be further studied in future work.

During plume modeling, the surrounding flow was considered stagnant. But in practice, the ocean is often density stratified in a non-linear and dynamic manner. In addition to this, currents are most of the time neither steady nor uniform. The interaction of turbulent flows driven by the sources of buoyancy with the surround-

ing flow is described as plumes in crossflow. The source in involve an additional parameter u_c, the crossflow velocity. Further studies could be made to compute the trajectory and mixing of these plumes based on the numerical integral analysis.

References

Abraham, G. (1963). Jet diffusion in stagnant ambient fluid. *Delft University of Technology*.

Ansong, J. K. (2009). Plumes in stratified environment. *University of Alberta*, page 167.

Aure, J. and Stigebrandt, A. (1989). On the influence of topographic factors upon the oxygen consumption rate in sill basins of fjords. *Estuarine, Coastal and Shelf Science*, 28:59–69.

Batchelor, G. (1954). Heat convection and buoyancy effects in fluids. *Quarterly Journal of the Royal Meteorological Society*, 80.

Bhamidipati, N. and Woods, A. W. (2017). On the dynamics of starting plumes. *Journal of Fluid Mechanics*, 833.

Briggs, G. A. (1970). A pume rise model compared with observations. *Journal of the Air Pollution Control Association*, page 70.

Bursik, M., Sparks, R. S. J., Gilbert, J. S., and Carey, S. (1992). Sedimentation of tephra by volcanic plumes: I. theory and its comparison with a study of the fogo a plinian deposit, sao miguel (azores). *Bulletin of volcanology*, pages 329–344.

Caulfield, C. and Woods, A. (1998). Turbulent gravitational convection from a point source in a non-uniformly stratified environment. *Journal of Fluid mechanics*, 360:229–248.

Devenish, B., Rooney, G., and Thomson, D. (2010). Large-eddy simulation of a buoyant plume in uniform and stably stratified environments. *Journal fo Fluid Mechanics*, 652:75–102.

Fischer, H. B., Koh, J. E. L. C. R., Imberger, J., and Brooks, N. H. (1979). *Mixing in Inland and Coastal Waters*. Academic Press, An Imprint of Elsevier.

Golmen, L. (1998). Artificial pumping of seawater in fjords. a preliminary feasibility study of a self-sustained diffusive pump.

Henderson-Sellers, B. (1983). The zone of flow establishment for plumes with significant buoyancy. *Applied Mathematics Modeling*, 7:395–397.

Hunt, G. R. and Kaye, N. G. (2001). Virtual origin correction for lazy turbulent plumes. *Journal of Fluid Mechanics*, Volume 435:pp. 377–396.

Kaye, N. B. (2008). Turbulent plumes in stratified environments: A review of recent work. *Atmosphere-Ocean*, 46:4.

Lee, J. and Chu, V. (2003). *Turbulent Jets and Plumes - A Lagrangian Approach.* Kluwer Academic Publishers.

McClimans, T., Eidnes, G., and Aure, J. (2002). Controlled artificial upwelling in a fjord using a submerged fresh water discharge: Computer and laboratory simulations. *Hydrobiologia*, 484:191–202.

Morton, B., Taylor, G., and Turner, J. S. (1956). Turbulent gravitational convection from maintained and instantaneous sources. *Proceedings of the Royal Society of London. Series A, Mathematical and Physical Sciences*, 234(1196)(1-23).

Morton, B. R. (1959b). Forced plumes. *Journal of Fluid Mechanics*, 5.

Nagamatsu, T. and Shima, N. (2006). Experimental study on artificial upwelling device combined v-shaped structure with flexible underwater curtain. *Memoirs of Faculty of Fsheries Kagoshima University*, 55.

Papanicolaou, P. N. and List, E. J. (1988). Investigations of round vertical turbulent buoyant jets. *Journal of Fluid Mechanics*, 195:341–391.

Rooney, G. and Devenish, B. (2014). Plume rise and spread in a linearly stratified environment. *Geophysical and Astrophysical Fluid Dynamics.*

Rouse, H., Yih, C. S., and Humphreys, H. W. (1952). Gravitational convection from a boundary source. *Tellus*, 4.

Saltelli, A., Ratto, M., Andres, T., Campolongo, F., Cariboni, J., Gatelli, D., Saisana, M., and Tarantola, S. (2008). *Global Sensitivity Analysis. The Primer.* John Wiley & Sons Ltd.

Scase, M. and Hewitt, R. (2011). Unsteady turbulent plume models. *Journal of Fluid Mechanics.*

Schlichting, H. (1979). *Boundary-layer theory.* McGraw-Hill.

Soltveit, T. and Jensen, P. M. (2017). Bunnvannet i Masfjorden må skiftes ut, mener hi-forskere.

Sparks, R. (1986). The dimensions and dynamics of volcanic eruption columns. *Bulletin of Volcanology*, 48:3–15.

Tennekes, H. and Lumley, J. (1994). *A First Course in Turbulence*. The MIT Press.

Turner, J. (1979). *Buoyancy Effects in Fluids*. Cambridge University Press.

Tzou, C.-N. (2015). Formation of underwater plumes and velocity variations due to entrainment in stratified environment.

Wong, D. and Wright, S. (1988). Submerged turbulent jets in stagnant linearly stratified fluids. *Journal of Hydraulic Research*, 26(1).

Yih, C.-S. (2012). *Stratified Flows*. Elsevier.

Yiwen, P., Wei, F., Dahai, Z., Jiawang, C., Haocai, H., Shuxia, L., Zongpei, J., Yanan, D., Mengmeng, T., and Ying, C. (2016). Research progress in artificial upwelling and its potential environmental effects. *Science China, Earth science*, 59:236–245.

Zeldovich, Y. (1937). The asymptotic laws of freely-ascending convective flows. *In Selected Works of Yakov Zeldovich*, 1.

Appendix A

A.1 Derivation of Reynolds average for the radial momentum equations

Considering the vertical axisymmetric plume, the sum of the turbulent mean and the fluctuating velocities in both vertical and radial directions respectively can be given as:

$$W(t) = w(t) + w(t)' \tag{A.1}$$

$$V(t) = v(t) + v(t)' \tag{A.2}$$

For simplification, we rewrite the Equation 2.8 which is the radial momentum equation

$$\rho\Big(\frac{\partial V}{\partial t} + V\frac{\partial V}{\partial r} + W\frac{\partial V}{\partial z}\Big) = -\frac{\partial p}{\partial r} \tag{A.3}$$

Multiplying the continuity equation by V which is given by Equation 2.12

$$V\left(\frac{\partial V}{\partial r} + \frac{\partial w}{\partial z}\right) = 0 \tag{A.4}$$

Adding with Equation A.3 and applying product rule, we come up with

$$\frac{\partial V}{\partial t} + \frac{\partial V^2}{\partial r} + \frac{\partial (VW)}{\partial z} = -\frac{1}{\rho}\frac{\partial p}{\partial r} \tag{A.5}$$

By taking the time average (i.e integrating the equation over time and dividing it again by time), we will have

$$\frac{\partial \overline{V^2}}{\partial r} + \frac{\partial (\overline{VW})}{\partial z} = -\frac{1}{\rho}\frac{\partial p}{\partial r} \tag{A.6}$$

Substituting the expression for V and W from Equation A.1 - A.2 and noting the fact that ($\overline{u'} = 0$, $\overline{\overline{u}} = \overline{u}$)

$$\frac{\partial v^2}{\partial r} + \frac{\partial \overline{(v')^2}}{\partial r} + \frac{\partial (vw)}{\partial z} + \frac{\partial (\overline{v'w'})}{\partial z} = -\frac{1}{\rho}\frac{\partial p}{\partial r} \tag{A.7}$$

$$\text{Since } \frac{\partial (vw)}{\partial z} = v\frac{\partial w}{\partial z} + w\frac{\partial v}{\partial z}$$
$$\frac{\partial v^2}{\partial r} = 2v\frac{\partial v}{\partial r}$$

Then, Equation A.7 becomes

$$2v\frac{\partial v}{\partial r} + v\frac{\partial w}{\partial z} + w\frac{\partial v}{\partial z} + \frac{\partial (\overline{v'w'})}{\partial z} = -\frac{1}{\rho}\frac{\partial p}{\partial r} - \frac{\partial \overline{(v')^2}}{\partial r} \tag{A.8}$$

By multiplying the time averaged continuity equation by v, we will get

$$v\left(\frac{\partial v}{\partial r} + \frac{\partial w}{\partial z}\right) = 0 \tag{A.9}$$

Subtracting Equation A.8 with Equation A.9 and doing some rearrangement, leads to the following Reynolds average radial momentum equation

$$\rho\left(v\frac{\partial v}{\partial r} + w\frac{\partial v}{\partial z}\right) = -\frac{\partial p}{\partial r} - \rho\left(\frac{\partial \overline{(v')^2}}{\partial r} + \frac{\partial (\overline{v'w'})}{\partial z}\right) \tag{A.10}$$

A.2 Derivation of Reynolds average for the vertical momentum equations

The technique engaged in the derivation of time-averaged vertical momentum equation is similar to Section **A.1**. The main difference is that the effects of body forces which is gravity in this case is considered. The vertical momentum equation can be written as:

$$\rho\Big(\frac{\partial V}{\partial t} + V\frac{\partial W}{\partial r} + W\frac{\partial W}{\partial z}\Big) = -\frac{\partial p}{\partial z} - g\rho \tag{A.11}$$

Multiplying Equation 2.12 by W and adding with A.11 gives us:

$$\frac{\partial V}{\partial t} + 2W\frac{\partial W}{\partial z} + V\frac{\partial W}{\partial r} + W\frac{\partial V}{\partial r} = -\frac{1}{\rho}\frac{\partial p}{\partial z} - g \tag{A.12}$$

By applying the product rule, we will get

$$\frac{\partial V}{\partial t} + \frac{\partial W^2}{\partial z} + \frac{\partial (VW)}{\partial r} = -\frac{1}{\rho}\frac{\partial p}{\partial z} - g \tag{A.13}$$

Applying time average on the above equation will give us:

$$\frac{\partial \overline{W^2}}{\partial z} + \frac{\partial(\overline{VW})}{\partial r} = -\frac{1}{\rho}\frac{\partial p}{\partial z} - g \tag{A.14}$$

Substituting the values of V and W from Equations A.1 - A.2

$$\frac{\partial w^2}{\partial z} + \frac{\partial \overline{(w')^2}}{\partial z} + \frac{\partial(vw)}{\partial r} + \frac{\partial(\overline{v'w'})}{\partial r} = -\frac{1}{\rho}\frac{\partial p}{\partial z} - g \tag{A.15}$$

After applying product rule

$$2w\frac{\partial w}{\partial z} + v\frac{\partial w}{\partial r} + w\frac{\partial v}{\partial r} + \frac{\partial(\overline{v'w'})}{\partial r} = -\frac{1}{\rho}\frac{\partial p}{\partial z} - \frac{\partial \overline{(w')^2}}{\partial z} \tag{A.16}$$

The continuity equation multiplied with w is

$$w\left(\frac{\partial v}{\partial r} + \frac{\partial w}{\partial z}\right) = 0 \tag{A.17}$$

Subtracting Equation A.17 from Equation A.16 and doing some rearrangement, leads to the following Reynolds average momentum equation towards the vertical direction

$$\rho\left(v\frac{\partial w}{\partial r} + w\frac{\partial w}{\partial z}\right) = -\frac{\partial p}{\partial z} - g\rho - \rho\left(\frac{\partial \overline{(w')^2}}{\partial z} + \frac{\partial(\overline{v'w'})}{\partial r}\right) \tag{A.18}$$

A.3 Density profiles in fjords

Depth(m)	Density ($\frac{kg}{m^3}$)
2	17.2731684
3	17.1649375
5	21.43455647
7	22.4140625
10	23.86332207
15	24.3746967
20	24.70487685
25	24.6003125
30	24.8933125
40	25.42772826
50	26.03220776
60	26.439625
70	26.8151875
80	26.86830797
90	27.1949375
100	27.34406944
125	27.5551875
150	27.728625
160	27.23423729
175	27.88542857
200	27.75249049
225	28.1025
250	28.2415
275	28.37
300	28.05366667
325	28.6565
350	28.7755
375	28.898
400	29.013

Table A.1: Density profiles with respect to depth in fjords. Measurements which is provided by NORCE (Norwegian Research Center) were made between 2011-2016.

Appendix B

B.1 Maximum height of plume rise

As stated in Equation 3.25, the maximum height attained by the plume rise is given as

$$z_{max} = \frac{\sqrt{2}}{\sqrt{\beta}\pi^{1/4}}\left(\frac{F_0}{N}\right)^{1/4}\left(\int_0^{\pi/N}\sqrt{\sin{(Nt)}}\,dt\right) \tag{B.1}$$

By applying substitution $u = Nt$, we have

$$z_{max} = \frac{\sqrt{2}}{\sqrt{\beta}\pi^{1/4}}\left(\frac{F_0}{N^3}\right)^{1/4}\left(\int\sqrt{\sin\,u}\,du\right)^{1/2} \tag{B.2}$$

Again let's sin $u = x^2$, $u = \sin^{-1}x^2$ and $du = \frac{dx}{\sqrt{1-x^4}}$. This leads to

$$z_{max} = \frac{\sqrt{2}}{\sqrt{\beta}\pi^{1/4}}\left(\frac{F_0}{N^3}\right)^{1/4}\left(\int\frac{x\,dx}{\sqrt{1-(x^2)^2}}\right)^{1/2} \tag{B.3}$$

Let's put again $x^2 = y$ and $xdx = \frac{dy}{2}$. Then we have

$$z_{max} = \frac{\sqrt{2}}{\sqrt{\beta}\pi^{1/4}}\left(\frac{F_0}{N^3}\right)^{1/4}\left(\frac{1}{2}\int\frac{dy}{\sqrt{1-y^2}}\right)^{1/2} \tag{B.4}$$

One more substitution, $y = \sin m$, $dy = \cos m\,dm$, then it become

$$z_{max} = \frac{\sqrt{2}}{\sqrt{\beta}\pi^{1/4}}\left(\frac{F_0}{N^3}\right)^{1/4}\left(\frac{1}{2}\int\frac{\cos m\,dm}{\sqrt{1-\sin^2 m}}\right)^{1/2} \tag{B.5}$$

$$= \frac{\sqrt{2}}{\sqrt{\beta}\pi^{1/4}}\left(\frac{F_0}{N^3}\right)^{1/4}\left(\frac{1}{2}\int dm\right)^{1/2} \tag{B.6}$$

$$= \frac{\sqrt{2}}{\sqrt{\beta}\pi^{1/4}}\left(\frac{F_0}{N^3}\right)^{1/4}\left(\frac{m}{2}\right)^{1/2} \tag{B.7}$$

By substituting back the value of m, we have

$$z_{max} = \frac{\sqrt{2}}{\sqrt{\beta}\pi^{1/4}} \left(\frac{F_0}{N^3}\right)^{1/4} \left(\frac{1}{2}\sin^{-1} y\right)^{1/2} \tag{B.8}$$

Again by substituting the value of y, we can get

$$z_{max} = \frac{\sqrt{2}}{\sqrt{\beta}\pi^{1/4}} \left(\frac{F_0}{N^3}\right)^{1/4} \left(\frac{1}{2}\sin^{-1} x^2\right)^{1/2} \tag{B.9}$$

$$= \frac{\sqrt{2}}{\sqrt{\beta}\pi^{1/4}} \left(\frac{F_0}{N^3}\right)^{1/4} \left(\frac{1}{2}\sin^{-1}\sin u\right)^{1/2} \tag{B.10}$$

$$= \frac{\sqrt{2}}{\sqrt{\beta}\pi^{1/4}} \left(\frac{F_0}{N^3}\right)^{1/4} \left(\frac{u}{2}\right)^{1/2} \tag{B.11}$$

After simplifying the equation, we finally come up with the final result

$$z_{max} = \frac{\pi^{1/4}}{\sqrt{\beta}} F_0^{1/4} N^{-3/4} \tag{B.12}$$

Appendix C

C.1 Matlab codes used in implementation of the mathematical model

We have used different Matlab code and scripts in the making of this master's thesis. The relevant part of the codes in its entirety with detailed comments is presented below. It should be noted that there are more codes and scripts in the thesis than those listed below.

C.1.1 Volume, momentum and buoyancy flux

```
%Volume, momentum and buoyancy flux calculations
zspan=[0 400];          %Height
v0mat = [q m b];        %Fluxes initial values

global g alpha rho0

g= 9.8;                 %Gravity
alpha = 0.116;          %Entrainment constant
rho0=29;                %Reference density, i.e density at z =0

zsol = {};              %Cell array initializations
v1sol = {};
v2sol = {};
v3sol = {};

%ODE solver
options=odeset('RelTol',1e-2,'AbsTol',1e-6,'Events',@events)
    ;
```

```
for k=1:size(v0mat,1) %ODE 45 solver in the cell array
   v0=v0mat(k,:);
   [z,v]=ode45(@rhs,zspan,v0,options);
   zsol{k}=z;
   v1sol{k}=v(:,1);
   v2sol{k}=v(:,2);
   v3sol{k}=v(:,3);
end

function [rho, Nsqr]=density1(z) %Output is buoyancy
    frequency

[~]=density1(z);

zvala=400-zval;
zvalue=fliplr(zvala);

rho2=fliplr(rho1);
rho3=smoothdata(rho2,'lowess',6);
rho=interp1(zvalue,rho3,z);
rho4=interp1(zvalue,rho3,z+0.1);

Nsqr=(-g./rho0).*(rho4-rho);

end
%% ODE volume, momentum and buoyancy flux equations

function parameters=rhs(z,v)

[~,Nsqr]=density1(z);

        dV= 2*alpha*sqrt(v(2));
        dM= (v(1).*v(3))./v(2);
        dF= -Nsqr.*v(1);

     parameters=[dV;dM;dF];

end
```

```
%% Stopping function
function [value, terminate, direction] = events(z,v)
    value = [v(1);v(2)];
    terminate = [1;1];
    direction = [0;0];
end
%Plots
 for k=1:size(v0mat,1)
%Volume flux plot
    figure(1)
      plot(abs(v1sol{k}),abs(zsol{k}),'k')
       hold on
        xlabel('Q (m^3/s)')
        ylabel('z (m)')
        grid on ;
 %Momentum flux plot
    figure(2)
      plot(abs(v2sol{k}),zsol{k},'r')
      hold on
        xlabel('M (m^4/s^2)')
        ylabel('z (m)')
        grid on
%Buoyancy flux plot
    figure(3)
      plot(abs(v3sol{k}),zsol{k},'r')
      hold on
        xlabel('F (m^4/s^3)')
        ylabel('z (m)')
       grid on
end
```

C.1.2 Maximum real height vs Briggs maximum height

```
%Maximum height vs Briggs height

zspan=[0 400]; %Height

y0mat=[b1*b1*w1 b1*b1*w1*w1 b1*b1*w1*g1;
       b2*b2*w2 b2*b2*w2*w2 b2*b2*w2*g2
       b3*b3*w3 b3*b3*w3*w3 b3*b3*w3*g3
       b4*b4*w4 b4*b4*w4*w4 b4*b4*w4*g4]; %Initial values

global g alpha rho0

g= 9.8;                 %Gravity
alpha = 0.116;          %Entrainment constant
rho0=29;                %Reference density, i.e density at z
   =0

zsol = {}; %Cell array initializations
v1sol = {};
v2sol = {};
v3sol = {};
mssflx={};              %Mass flux
gmark={};               %Reduced gravity
vel={};                 %Vertical velocity
b={};                   %Width
mntflx={};              %Momentum flux
bncyflx={};             %Buoyancy flux

options=odeset('RelTol',1e-7,'AbsTol',1e-7,'Events',
   @stopevents); %ODE 45 solver

 for k=1:size(y0mat,1) %ODE 45 solver in the cell array
  y0=y0mat(k,:);
  [z,y]=ode45(@rhs,zspan,y0,options);
  zsol{k}=z;
  v1sol{k}=y(:,1);
  v2sol{k}=y(:,2);
  v3sol{k}=y(:,3);
```

```
    mssflx{k} =y(:,1);
    vel{k}=y(:,2)./mssflx{k};
    gmark{k}=y(:,3)./mssflx{k};
    b{k}=sqrt(mssflx{k}./vel{k});
    mntflx{k}=mssflx{k}.*vel{k};
    bncyflx{k}=mssflx{k}.*gmark{k};

    ZH{k}=5*pi*b{k}.*b{k}.*vel{k}.*gmark{k};%Maximum height

end

function [rho, Nsqr]=density1(z) %Output is buoyancy
    frequency

[~]=density1(z);

zvala=400-zval;
zvalue=fliplr(zvala);

rho2=fliplr(rho1);
rho3=smoothdata(rho2,'lowess',6);
rho=interp1(zvalue,rho3,z);
rho4=interp1(zvalue,rho3,z+0.1);

Nsqr=(-g./rho0).*(rho4-rho);

end

%%The main function equations

function dy=rhs(z,y)

[~, Nsqr]=density1(z);

massflux=y(1);
velocity=y(2)/massflux;
gmark=y(3)/massflux;
fric= 1*velocity*abs(velocity);  %Friction
```

```
b=sqrt(massflux/velocity);
ZH=3.76*pi*b^2.*velocity*gmark;  %Maximum height

dy(1)=2*alpha*b*velocity;
dy(2)=b*b*gmark- fric;
dy(3)=-massflux*Nsqr*Nsqr;
dy=dy';
end

%%Stop function

function [val, terminate, dir]= stopevents(t,y)
val=y(2);
terminate=1;
dir=0;
end

%Plots and scatters

for r=1:length(ZH)  %Initialization
q(r)=r;
end

for k2 = 1:length(ZH)
 Mzsol(k2) = max(real(ZH{k2}));  %Briggs height
end

 for k1 = 1:length(vel)
  zsol04(k1) = interp1(real(vel{k1}), real(zsol{k1}),0.0001)
      ; %Maximum height
 end
```

C.1.3 Numerical calculation of the entrainment coefficient, α

```
zspan=[0,400];
v0mat = [0.9  0.01  0.9];%Initial values
tol = 10^-7; % Treshold
MAX = 1000;%Maximum iteration
v2 = 0.01;%Reference value
interval = [0.01  0.09]; %Alpha interval
a = interval(1);
b = interval(2);
alpha = (a+b)/2;
zsol = {};%Cell array initializations
v1sol = {};
v2sol = {};
v3sol = {};
for k=1:size(v0mat,1)
   v0=v0mat(k,:);
   [z,v]=ode45(@(z,v)rhs(z,v,alpha),zspan,v0);
   zsol{k}=z;
   v1sol{k}=v(:,1);
   v2sol{k}=v(:,2);
   v3sol{k}=v(:,3);
end
iter = 1;
while(abs((v(:, 2)) - v2) > tol)
 alpha= (a + b)/2;
[z,v]=ode45(@(z,v)rhs(z,v,alpha),interval,v0);
 if(abs(v(end,2))-v2 > 0)
b = alpha;
 else
 a = alpha;
 end
 iter = iter + 1;
 if(iter > MAX)
 return;
 end
end
function parameters=rhs(z,v,alpha)
              Nsqr = 0.01;
```

```
        db= 2*alpha-(v(1).*v(3))./(2*v(2).^2);
        dw= (v(3)./v(2))-(2*alpha*v(2)./v(1));
        dgmark= -Nsqr-(2*alpha*v(3)./v(1));
    parameters=[db;dw;dgmark];
end
```

C.1.4 3D Plume modeling by assuming the buoyancy frequency, N = 10^{-2}

```
clear
zspan = linspace(0,2,100);
v2in_vals = linspace(0.01,0.05,10);
v1in_vals = linspace(0.01,0.05,10);
v3in_vals = linspace(0.01,0.05,10);
v0mat = [1  0.1  1];
N = size(v0mat, 1);
zsol = cell(N,1); %Cell array initilaization
v1sol = cell(N,1);
v2sol = cell(N,1);
v3sol = cell(N,1);
v1in = cell(N,1);
v2in = cell(N,1);
v3in = cell(N,1);

for k=1:length(v2in_vals)
  v0 = v0mat;
  v0(2) = v2in_vals(k);
  [z,v] = ode45(@rhs,zspan,v0);
  zsol{k} = z;
  v1sol{k} = v(:,1);
  v2sol{k} = v(:,2);
  v3sol{k} = v(:,3);
  v2in{k} = v0mat(2) * ones(size(v2sol{k}));
  v1in{k} = v0mat(1) * ones(size(v1sol{k}));
  v3in{k} = v0mat(1) * ones(size(v3sol{k}));
end
all_z = [zsol{:}];
all_v1 = [v1sol{:}];
all_v1in = [v1in{:}];
```

```
all_v2 = [v2sol{:}];
all_v2in = [v2in{:}];
all_v3 = [v3sol{:}];
all_v3in = [v3in{:}];
%Width
figure(1)
subplot(1,2,1);
plot3(all_v1, all_z,all_v1in);
xlabel('b')
ylabel('z')
zlabel('db')
grid on

subplot(1,2,2)
v1in_vec = v1in_vals;
z_vec = all_v1(:,1);
surf(z_vec, v1in_vec, all_v1.')
xlabel('z');
ylabel('db');
zlabel('b');

%Vertical velocity
figure(2)
subplot(1,2,1);
plot3(all_v2, all_z, all_v2in);
xlabel('w')
ylabel('z')
zlabel('dw')
grid on

subplot(1,2,2)
v2in_vec = v2in_vals;
z_vec = all_v2(:,2);
surf(z_vec, v2in_vec, all_v2.')
xlabel('z');
ylabel('dw');
zlabel('w');

figure(3)
```

```
subplot(1,2,1);
plot3( all_z, all_v3in, all_v3.');
xlabel('g''')
ylabel('z')
zlabel('dg''')
grid on

subplot(1,2,2)
v3in_vec = v3in_vals;
z_vec = all_v3(:,3);
surf(z_vec, v3in_vec, all_v3.')
xlabel('z');
ylabel('dg''');
zlabel('g''');

function parameters=rhs(z,v)
            alpha=0.116;
            db= 2*alpha-(v(1).*v(3))./(2*v(2).^2);
            dw= (v(3)./v(2))-(2*alpha*v(2)./v(1));
            dgmark= -0.01-(2*alpha*v(3)./v(1));
   parameters=[db;dw;dgmark];
  end
```